Published in final edited form as:
Nat Prod Rep. 2009 May ; 26(5): 585–601. doi:10.1039/b813799b.

Isolation, biology and chemistry of the disorazoles: new anti-cancer macrodiolides

Chad D. Hopkins and **Peter Wipf**
Department of Chemistry, University of Pittsburgh, Pittsburgh, Pennsylvania 15260, U. S. A.

Abstract

The disorazoles comprise a family of 29 closely related macrocyclic polyketides isolated in 1994 from the fermentation broth of the gliding myxobacterium *Sorangium cellulosum*. Disorazoles A_1, E and C_1 have shown exceptional biological activities toward inhibiting the proliferation of human cancer cell lines in picomolar and nanomolar concentrations through the disruption of microtubule polymerization. This review gives a brief introduction describing the biosynthesis and the significance of the disorazoles as a new class of microtubulin disruptors. Another portion of the review focuses on the biology of the disorazoles, specifically disorazole A_1 and C_1, and their antiproliferative efficacy against animal and human tumor cell lines, as well as the available SAR data. The majority of the discussion addresses synthetic efforts, including partial syntheses of various disorazoles and a summary of the total synthesis of disorazole C_1.

1 Introduction

Natural products present us with a treasure trove of structurally novel and mechanistically inspiring biologically active agents and, occasionally, even therapeutic drugs. The disorazoles comprise a new class of microtubule disrupting cytotoxic macrodiolides isolated from the fermentation broth of the myxobacterium *Sorangium cellulosum* So ce12. These secondary metabolites show exceptional subnanomolar activity against a panel of cancer cell lines and have a mode of action related to but not identical to that of vinca alkaloids. The blend of intriguing biological potency along with the complex and unusual molecular architecture of the disorazoles has triggered the curiosity of biologists and synthetic chemists alike.

In this review, the isolation and current information regarding the biosynthesis and biological target of the disorazoles will be discussed. Biological data for the disorazoles are summarized and compared to known anti-cancer agents such as the vinca alkaloids, dolastatins, and epothilones. In addition, synthetic efforts including partial syntheses and the total synthesis of disorazole C_1 will be addressed in detail. A brief overview of published efforts toward the syntheses of disorazoles A_1 and D_1 will also be presented.

2 Isolation, structure and biosynthesis

The disorazoles comprise a family of 29 macrodiolides first isolated in 1994 by Jansen, Irschik, Reichenbach, Wray and Höfle from the fermentation broth of the gliding bacteria (myxobacteria) strain *Sorangium cellulosum* So ce12.[1] Myxobacteria exhibit features of both unicellular and multicellular organisms and have a history of producing a rich collection of biologically active secondary metabolites,[2] including the epothilones,[3] chondramide B,[4] apicularen,[5] gephyronic acid,[6] rhizopodin,[7] and tubulysins.[8] These “slime bacteria” travel by gliding, or creeping, in waves across the surface of a host and are found in soil, rotting plant material, animal dung, and on the bark of living and dead trees.[9]

The disorazoles were isolated from the original fermentation broth by solvent partition and chromatographic separation. Disorazole A_1 was identified as the major component, comprising 69.8% of the relative mass amount compared to the remaining 28 disorazoles (Fig. 1). Disorazole A_1 was also used as the basis for the structure elucidation of the disorazoles. Its molecular formula was determined by negative and positive ion FAB mass spectrometry, high-resolution mass spectrometry, and elemental analysis. Major structural subunit determinations and further structure refinements were achieved using 1D and 2D NMR techniques. The isolation group reported that the disorazoles were stable during the purification process, and, most importantly, that disorazole A_1 (**1**) was not contaminated with disorazole D_1 (**6**) after chromatography with aqueous methanol, indicating that the epoxide of disorazole A_1 was not readily opened to form the diol group in disorazole D_1.[1] However, the possibility that several of the minor members of this family are artefacts derived from side reactions such as olefin isomerization or epoxide solvolysis during the isolation and purification process cannot be completely excluded.

The potential therapeutic value of the disorazoles was highlighted by the identification of the biosynthetic gene cluster by an industrial group in 2005.[10,11] Interestingly, the DisA gene does not contain a loading domain to transfer acetyl-CoA or malonyl-CoA to an acyl carrier protein (ACP) (Fig. 2). The most likely scenario to explain the initiation of the biosynthesis involves a direct transfer of an acetyl group from CoA onto the ketosynthase (KS) module.[10,11] The geminal methyl groups at C-15 and C-15′ are derived from *S*-adenosyl methionine based on ^{13}C-labelled methionine feeding studies,[1] and are consistent with the presence of a methyltransferase (MT). The purpose of the second ACP in module 2 is not clear as it lacks the active site serine for 4′-phosphopantetheine addition. The β-hydroxyl group at C-14 and C-14′ is installed at module 3 *via* the KS, β-ketoreductase (KR), and ACP domains. Chain extension occurs at the DisB site through a series of KS, β-hydroxydehydrase (DH), KR, and ACP domains to afford the conjugated polyene unit observed in the disorazoles. The point at which the hydroxyl group at C-6 is installed remains a subject of debate. The DH domain at module 7 may remain either continuously active to produce an intermediate containing four conjugated double bonds, with the hydroxyl group being installed during post PKS synthetic steps, or, alternatively, the DH domain at module 7 may function only half of the time. Obviously, the latter scenario is only one out of many alternative reasons for the formation of unsymmetrical macrodiolide products from two non-identical *seco*-acids. Ultimately, cyclization may be driven by conformational factors and/or ring strain, thus only allowing some combinations of *seco*-acids to cyclize. An interrupted process controlled by the seemingly unnecessary extension units might account for the diversity in *seco*-acid combinations. Similar mechanisms have been discussed in cyclopeptide biosynthesis. However, in the absence of any specific evidence to the contrary, the most likely hypothesis is the formation of a yet-to-be-identified symmetric macrodiolide that is subjected to post-PKS diversifications. Formation of an oxazolidine ring occurs at the DisC site *via* two heterocyclization (HC) domains. The first HC domain of the unusual dual HC domain may serve to incorporate serine, while the second HC domain promotes cyclization to the oxazoline. Alternatively, both steps may be catalyzed by the first HC domain while the second site remains inactive.[10] Oxidation of the oxazoline to the final oxazole heterocycle by the oxidation domain (Ox) of the DisC site completes the synthesis of the monomeric disorazole backbone. Modules 9 and 10 of DisD appear to be unnecessary for the synthesis of disorazole, and therefore the monomer could be released from the chain by the thioesterase (TE). Whether the TE of DisD participates in the dimerization of the biosynthetic monomer or the dimerization occurs *via* an alternative enzyme has yet to be determined. Further structural modifications required to construct the various members of the disorazole family are believed to occur post PKS.

3 Biological function

Soon after the initial isolation of the disorazoles in 1994,[1] biological follow-up studies revealed the exceptional cytotoxicity of these secondary metabolites in cell cultures as well as their antifungal effects. In contrast, disorazoles do not appear to possess potent antiviral or antibacterial activity.[12] To date, disorazole A_1 (**1**) remains the most extensively studied member of the disorazole family with regard to its biological activity and mode of action.[12-14] Mainly, this preference is due to its relatively large natural abundance in comparison to other disorazoles.[1] In 2004, Elnakady, Sasse, Lünsdorf and Reichenbach demonstrated that the antimitotic properties of disorazole A_1 originated from its tubulin polymerization inhibitory activity. They provided evidence that picomolar concentrations of disorazole A_1 were sufficient for destabilizing microtubule assembly, blocking mitosis, and inducing apoptosis. Additional studies supported that the disorazoles derived their tubulin depolymerization activity from binding to or near the vinca domain, thus resulting in an irreversible perturbation of the microtubule network as well as cell cycle arrest at the G_2/M checkpoint, and triggering of the apoptotic cell death cascade.[14]

The exposure of cells to agents that perturb the dynamic polymerization–depolymerization equilibrium of tubulin α,β-heterodimers results in dysfunctional mitotic spindles, which are critical for proper sister chromatid segregation, mitosis and the cytokinesis of dividing cells.[15] The potent bioactivity of the disorazoles mainly originates from their ability to disrupt microtubule formation; accordingly they share a mechanism of action found for the vinca alkaloids and other anticancer drugs, such as the lipophilic peptides dolastatin 15[16] and tubulysin A,[17] as well as the autumn crocus secondary metabolite colchicine.[18] In contrast, the clinically used taxanes[19] and epothilones,[20] as well as (+)-discodermolide,[21] dictyostatin,[22] laulimalide,[23] and other natural products,[24] derive their activity from the stabilization of microtubules (Fig. 3). Among the secondary metabolites isolated from myxobacteria, the disorazoles represent the third distinct class of compounds (in addition to epothilones and tubulysins) that interfere with microtubule dynamics.

Disorazole A_1 exhibits a concentration-dependent growth inhibition of the leukemia cell line L929 with an exceptionally potent IC_{50} value of 3 pM.[12,14] This disorazole has also shown remarkable inhibition properties towards numerous other human cancer cell lines. Compared to epothilone B and vinblastine, the antiproliferative efficacy of disorazole A_1 was superior in all cell-based studies by at least an order of magnitude.[14] Remarkably, disorazole A_1 retained its potency against the multi-drug resistant cell line KB-V1 which overexpresses the P-glycoprotein (Pgp) efflux pump (Table 1). Pgp is believed to function as an ATP-linked transporter for hydrophobic xenobiotics, and high expression levels of Pgp in tumors are often associated with a poor response to chemotherapeutic drugs, resulting in grave tumor prognosis.[25] While it remains to be established if the disorazoles share a mechanism-based neurotoxicity with other tubulin (de)stabilizing agents, their activity in a multidrug resistant cell line bodes well for potential future use in cancer therapy.

Comparatively few biological data are available for other disorazoles. Wipf, Graham, Vogt, Sikorski, Ducruet, and Lazo have demonstrated that disorazole C_1 (**10**) was an effective cytotoxic agent with IC_{50} values ranging from 1.6−6.9 nM in various human cancer cell lines (Table 2).[26] These results were comparable to IC_{50} values of the clinically used vinblastine and vincristine. Additionally, a high-content analysis of mitotic arrest in HeLa cells treated with disorazole C_1, vincristine, vinblastine, colchicine, and paclitaxel provided IC_{50} values of 14.6, 6.9, 0.3, 23.9, and 6.7 nM, respectively.[27] Remarkably, while the absence of the highly electrophilic vinyl oxirane at carbons 9 and 10 in disorazole C_1 reduced its cytotoxicity by 50−100 fold compared to disorazole A_1, the simplified macrodiolide is still an exceedingly potent

agent. Furthermore, disorazole C_1 was recently shown to induce premature senescence and may bind to a site distinct from the vinca alkaloids.[28]

Structure–activity relationship (SAR) studies performed on disorazole C_1 revealed that truncation or alteration of the backbone functionality was highly detrimental to the activity of the macrodiolide (Fig. 4).[26] The absence of the allylic alcohol side chain or incorporation of a cyclopropane alkene isostere destroyed all activity. Additionally, replacement of the triene unit with a dienyne yielded an analog exhibiting three orders of magnitude lower potency. Subunits of disorazole C_1 were completely inactive, and compounds lacking a methoxy group at C-6 were too unstable to isolate. Based on this information, it appears that the side chain functionalities as well as the distinct triene backbone are essential for adequate binding to the biological target, and necessary to exhibit potent antiproliferative activity. It is quite feasible that disorazole C_1 represents the minimum pharmacophore of the disorazole family. The final resolution of this puzzle will likely require the elucidation of the molecular mode of interaction of the disorazoles with the α,β-tubulin heterodimer.

4 Synthetic strategies

4.1 Meyers' partial synthesis of disorazole C_1

The disorazoles are a structurally novel class of macrocyclic polyketide microtubule disruptors. The presence of both heterocyclic and labile polyene linkages within the macrocyclic scaffold present the synthetic chemist with intriguing challenges. The C_2-symmetrical disorazole C_1 remains the simplest of the currently known disorazoles and was the first to be featured in synthetic studies by the Meyers group in 2000.[29] At the start of these investigations, neither the relative nor the absolute configuration of the disorazoles had been reported, resulting in an arbitrary initial selection of the stereochemical features of the target molecule.

Meyers' retrosynthetic approach involved a disconnection of the dimeric macrolactone to the triene monomer **14** which could be constructed through the joining of oxazole **16** and diol **15** *via* a Stille cross-coupling at carbons 10 and 11 (Fig. 5). The construction of the oxazole C-1 through C-10 segment began with the hydrolysis of the readily available ester **17** followed by coupling with a racemic serine methyl ester to afford the hydroxy amide **18** (Scheme 1). Subsequent diethylaminosulfurtrifluoride (DAST) mediated cyclodehydration followed by oxidation[30] provided oxazole **19** in 79% yield over two steps. Successive protecting group manipulations followed by Parikh–Doering oxidation of the resulting primary alcohol **20** afforded the desired aldehyde which was immediately submitted to a Wittig olefination to generate enal **21**. Finally, a Stork–Zhao olefination[31] in the presence of hexamethylphosphoramide (HMPA) provided the (*Z*)-vinyl iodide fragment **16** (*Z*/*E* = 18: 1) in 11 steps from ester **17**.

The synthesis of the C-11 through C-19 diol fragment **15** commenced with an enantioselective Mukaiyama aldol reaction between (*E*)-crotonaldehyde and the *O*-silyl ketene acetal **22** under Kiyooka's conditions[32] to afford acetal **23** in 73% yield and 92−93% ee based on Mosher ester analysis (Scheme 2). Silyl protection of the secondary alcohol **23** followed by acetal hydrolysis in the presence of 80% AcOH revealed the desired aldehyde **24**. Horner–Wadsworth–Emmons olefination of this aldehyde effectively installed an (*E*)-α,β-unsaturated ester that was immediately reduced in the presence of DIBAL-H to generate the allylic alcohol **25**. The remaining stereocenter at C-14 was installed *via* a Sharpless asymmetric epoxidation in a 15: 1 dr and in 95% yield with epoxide *26* representing the major product. Subsequent selective epoxide opening with Red-Al followed by diol protection afforded the acetal **27** in 83% yield over 2 steps. A regioselective ring opening of acetal **27** with DIBAL-H and Dess–Martin oxidation of the resulting primary alcohol gave aldehyde **28**. Stork–Zhao olefination[31] of aldehyde **28** followed by oxidative PMB cleavage in the presence of DDQ successfully

installed the (*Z*)-olefin geometry at carbons 11 and 12. The authors observed that the PMB protecting group had to be removed prior to the generation of the vinyl stannane due to a DDQ-mediated destannylation. Palladium-catalyzed deiodination/stannylation of vinyl iodide **29** followed by Stille coupling of the resultant vinyl stannane to the oxazole segment **16** completed the synthesis of the monomeric unit **14**. Unfortunately, the authors were unable to continue with the synthesis and effect the dimerization of **14**, possibly due to the instability of the labile triene unit.

In order to overcome the propensity of the triene unit at C-7 through C-12 to isomerize, Meyers investigated a second generation approach by masking the (*Z*)-alkene at C-11/C-12 as an alkyne (Scheme 3).[33] An approach similar to the one described in Scheme 2 was adopted to construct the requisite alkyne from acetal **23**. The authors found that by simply treating acetal **23** with 2.0 equivalents of NaH in the presence of triethylphosphonoacetate, direct access to the α,β-unsaturated ester **30** was achieved in 72% yield *via* an initial collapse of the acetal and a concurrent 1,5 O→O silyl migration,[34] resulting in the exclusive formation of the aldehyde (Scheme 3). This aldehyde was then free to participate in the subsequent *in situ* Horner–Wadsworth–Emmons olefination. Subjecting the α,β-unsaturated ester **30** to a similar series of reactions described in Scheme 2 (*vide supra*) provided (*Z*)-vinyl iodide **34** which smoothly underwent elimination in the presence of NaHMDS to afford the terminal alkyne **35** in 93% yield. Sonogashira cross-coupling with oxazole segment **16** provided dienyne **36** in 87% yield. However, upon hydrolysis of the methyl ester and treatment of the crude carboxylic acid with dipyridyl thionocarbonate (DPTC) in the presence of a catalytic amount of DMAP in toluene at reflux afforded exclusively the intramolecular cyclization product macrolactone **37**. Furthermore, changes in the reactant concentration did not influence the outcome of this reaction and no attempts to employ alternative macrolactonization conditions were made. The structural assignments of the synthetic intermediates were confirmed by a single crystal X-ray analysis of alcohol **38**.

The authors addressed the dimerization problem by adopting a stepwise coupling approach (Scheme 4). An orthogonal silyl protection of the secondary alcohol at C-14 of dienyne **36** followed by hydrolysis of the methyl ester afforded the corresponding carboxylic acid. Coupling to a second equivalent of alcohol **36** in the presence of DPTC and a catalytic amount of DMAP in toluene at reflux gave exclusively ester **39**. Selective removal of the secondary TES protecting group in the presence of TFA/H_2O (1: 1) in THF followed by saponification and Yamaguchi macrolactonization led to the desired bislactone **40** in a low 24% yield over the final two steps. Formation of a large amount (67%) of the lactone monomer **37** was also observed due to a non-selective ester hydrolysis of **39**. Attempts to overcome the problematic dimerization step were unsuccessful. Unfortunately, desilylation at C-16 and C-16′ of **40** was also unsuccessful and resulted in significant amounts of transesterification and decomposition products that were inseparable by column chromatography. Furthermore, partial reduction of the triple bonds at C-11/C-12 and C-11′/C-12′ was ineffective. In contrast, partial reduction of monomer **36** in the presence of Zn–Cu–Ag alloy in MeOH/H_2O at 80 °C for 48 h in a sealed tube afforded the triene in 91% yield accompanied by some olefin isomerization products (not shown).

4.2 Hoffmann's synthesis of tetradehydrodisorazole C_1

In 2000, the absolute and relative configuration of the disorazoles was assigned by Höfle through degradation studies of disorazole A_1 (**1**).[35] The stereochemical information gained from these studies was undoubtedly unavailable to Meyers and co-workers at the time of their work on disorazole C_1.[29,33] In 2002, Hoffmann and co-workers first reported the synthesis of a masked fragment of disorazole C_1 with the correct absolute and relative configurations at all stereocenters.[36] Hoffmann adopted a synthetic strategy that utilized a strategically placed

alkyne along the C-7/C-12 backbone to mask the labile triene moiety of disorazole C_1, thereby allowing for a more efficient cyclodimerization of dienyne **41** (Fig. 6).

The appropriate placement of an alkyne was expected to induce sufficient ring strain to suppress an intramolecular lactonization to the undesired 15-membered macrolactone. Force field energy minimizations revealed that positioning the alkyne at C-9/C-10 versus C-11/C-12 resulted in greater ring strain for the undesired 15-membered lactone (330.2 kJ/mol vs 245.0 kJ/mol, respectively) and a lower energy in the corresponding 30-membered lactone (465.8 kJ/mol vs 499.3 kJ/mol, respectively) (Fig. 7).[36] Additionally, positioning the alkyne at C-9/C-10 did not significantly affect the relative energies of tetradehydrodisorazole C_1 (**44**) and disorazole C_1 (465.8 kJ/mol vs 463.3 kJ/mol, respectively).

The synthesis of vinyl iodide **42** commenced with an asymmetric Mukaiyama aldol reaction under Kiyooka's conditions[32] to afford β-hydroxy ester **48** in 96% yield and 88% ee (Scheme 5). Protection of the secondary alcohol followed by sequential ester reduction and re-oxidation in the presence of Dess–Martin periodinane generated the desired aldehyde **49**. An attempted stereoselective addition of lithiated *trans*-bromopropene to aldehyde **49** proved problematic, resulting in a 1.1: 1.0 *syn*: *anti* mixture of separable diastereomers at C-16. Nonetheless, the *anti*-diol was carried forward an additional 4 steps to provide the orthogonally protected diol fragment **42**.

Oxazole **43** was constructed beginning with a Keck allylation[37] of the readily available aldehyde **52** in the presence of (*R*)-BINOL to afford the homoallylic alcohol **53** in 84% yield and >94% ee (Scheme 6). *O*-Methylation of the secondary alcohol **53** followed by ozonolysis and oxidation of the resulting aldehyde gave the corresponding carboxylic acid **54**. Coupling of **54** with L-serine methyl ester hydrochloride in the presence of isobutyl chloroformate (IBCF) and *N*-methylmorpholine (NMM) followed by DAST-mediated cyclodehydration and DBU/$BrCCl_3$ oxidation[30] of the resulting oxazoline yielded oxazole **55**. Debenzylation and subsequent oxidation of the primary alcohol **56** provided the desired aldehyde **57**. A three-carbon chain extension of aldehyde **57** *via* Wittig olefination with TMS-protected propargyl triphenylphosphonium bromide proceeded with poor olefin selectivity (*E*/*Z* = 2.5: 1.0) at C-8 and a moderate 49% yield. The inseparable alkene isomers were desilyated to provide the oxazole fragment **43** which was subsequently coupled to vinyl iodide **42** *via* a Sonogashira cross-coupling reaction to provide dienyne **41** in 58% yield followed by chromatographic separation of alkene isomers.

As a result of the problems associated with poor selectivity during the instalment of the (*E*)-alkene at C-7/C-8, Hoffmann devised a second generation approach that involved a double Sonogashira cross-coupling reaction to selectively construct carbon–carbon bonds at C-8/C-9 and C-10/C-11.[38] Oxidation of the primary alcohol **56** followed by immediate treatment of the resulting unstable aldehyde with the Ohira–Bestmann reagent **61** provided terminal alkyne **57** in 75% yield over 2 steps (Scheme 7). Alkyne **57** smoothly underwent hydrostannylation/iododestannylation to selectively afford the (*E*)-configured vinyl iodide **58** in 88% yield.

The enyne **59** coupling partner was easily obtained *via* a three-step sequence involving a Sonogashira cross-coupling with the previously synthesized vinyl iodide **42** and TMS-acetylene, followed by selective removal of the TMS and TBDMS protecting groups. With the newly prepared fragments in hand, vinyl iodide **58** and enyne **59** were coupled *via* a second Sonogashira reaction to afford the fully resolved dienyne **60** in 89% yield (Scheme 7). The authors found that removal of the TBDMS protecting group at C-14 was required early on, as late stage cleavage resulted in either no reaction or decomposition.[38]

With dienyne **60** in hand, a direct dimerization of the carboxylic acid derived from **60** was examined as part of the endgame strategy but was unsuccessful under a variety of conditions

(*e.g*. DPTC/DMAP, Yamaguchi, and 2-chloro-1-methylpyridinium iodide/DMAP).[38] Interestingly, formation of a 15-membered lactone resulting from monomer cyclization[33] was not observed, thereby emphasizing the utility of the alkyne placement within the masked triene subunit. A double Sonogashira approach was also briefly explored on a model system to effect the dimerization but met with failure (Scheme 8). In order to circumvent the difficulties encountered during the dimerization strategy, a lengthier, stepwise approach was pursued. Silyl protection of the free secondary alcohol of dienyne **60** with TESOTf followed by hydrolysis of the methyl ester and subsequent Yamaguchi esterification provided the desired ester in a moderate 69% yield (Scheme 9). The authors found that it was important to activate the free carboxylic acid portionwise in order to avoid decomposition of the acylating agent prior to the reaction with alcohol **60**. Subsequent cleavage of the silyl ether at C-14 proceeded in 87% yield followed by selective hydrolysis of the methyl ester in the presence of the internal ester linkage to furnish the corresponding acid quantitatively. Finally, Yamaguchi macrolactonization provided the *O*-silyl protected tetradehydrodisorazole C_1 **65** in a low 31% yield. Curiously, the authors did not report any attempts to remove the protecting groups of macrodiolide **65** to complete a formal total synthesis of disorazole C_1.[39]

4.3 Wipf's total synthesis of (−)-disorazole C_1

Although the constitution of the disorazoles has been known since 1994[1] and relative and absolute configurations for disorazole A_1 were assigned in 2000,[35] it was not until 2004 that a total synthesis of a member of the disorazole class was reported by Wipf and Graham.[39] Previous work by Meyers[29,33] and Hoffmann[36,40,41] revealed important synthetic parameters, including the instability of the triene backbone and the significance of the position of the alkyne which served both to mask the (*Z*)-olefin(s) of the triene unit as well as facilitate the macrolactonization. Wipf and Graham were able to capitalize on these important findings and devise a synthetic approach that utilized a Sonogashira coupling to construct the carbon–carbon bonds at C-8/C-9 of the dienyne monomer **66** (Fig. 8). Easily under-appreciated but most significant for the success of this synthesis was the selection of a *p*-methoxybenzyl protecting group for the hydroxyl function at C-16. Due to the sensitive nature of the late stage intermediates, the oxidative but relatively neutral conditions used for PMB removal were superior to basic, fluoride, or acidic conditions. Key fragments **67** and **58** would be derived from known alcohol **68**[42] and alkyne **69**, respectively.

The synthesis of oxazole fragment **58** commenced with the *O*-silyl protection of hydroxy nitrile **70** followed by partial reduction of the nitrile to afford aldehyde **71** in 78% over two steps (Scheme 10). Alkyne addition to aldehyde **71** was performed under Pu's conditions[43] to provide the propargyl alcohol in 66% yield and 92% ee. Other asymmetric alkyne transfer conditions were tried but provided inferior results, in agreement with the findings of Marshall.[44] *O*-Methylation of the secondary alcohol under phase-transfer conditions proceeded with concomitant removal of the TMS group to provide the terminal alkyne **69** in 95% yield. Cleavage of the silyl ether followed by oxidation of the resulting primary alcohol under conditions developed by Merck[45] afforded carboxylic acid **72** in excellent yield. Hydroxy amide formation followed by DAST-mediated cyclodehydration and subsequent $BrCCl_3$/DBU oxidation[30] yielded a mixture of bromoalkyne **73** and terminal alkyne **74**. Both compounds were converted to the (*E*)-vinyl iodide **58** through a palladium-catalyzed hydrostannylation/iododestannylation sequence, with the bromoalkyne showing greater selectivity. Accordingly, terminal alkyne **74** was further converted to the bromoalkyne **73** in the presence of NBS and $AgNO_3$ in acetone in a moderate 54% yield. Finally, hydrolysis of the methyl ester completed the synthesis of oxazole fragment **75**.

The key enyne **67** was obtained from the readily available homoallylic alcohol **68**[42] in 13 overall steps (Scheme 11). Ozonolysis of alkene **68** followed by reductive work-up with

$NaBH_4$ afforded the corresponding alcohol. 1,3-Diol protection followed by hydrolysis of the naphthyl ester provided acetonide **76**. Swern oxidation of the primary alcohol proceeded smoothly, but, unfortunately the subsequent alkyne addition using 1-lithiopropyne proved problematic, resulting in formation of a 1.1: 1.0 (*syn: anti*) ratio of separable diastereomers at C-16. Hoffmann also reported difficulties in the selective formation of the neopentyl *anti*-1,3-diol.[36,41,46] Attempts at improving the diastereoselectivity for the generation of this diol segment have thus far proved unsuccessful. Nevertheless, the *anti*-1,3-diol **78** was carried forward to provide diol **79** *via* alkyne reduction using Red-Al in degassed THF followed by PMB protection of the resulting allylic alcohol and subsequent acetonide cleavage. Protection of the free hydroxyl groups with TESOTf and selective Swern oxidation of the primary silyl ether gave aldehyde **80** in 75% yield over two steps. With aldehyde **80** in hand, Wipf utilized a Peterson olefination in the presence of Corey's lithiated 1,3-bis(triisopropylsilylpropyne)[47] to install the (*Z*)-alkene at C-11/C-12 to afford, upon selective cleavage of the TES ether, enyne **81** as a separable 8: 1 (*Z/E*) mixture in 62% overall yield over two steps. Completion of enyne fragment **67** was successfully accomplished in 94% yield *via* a TIPS-deprotection of enyne **81**.

The two coupling components, oxazole **58** and enyne **67**, were subjected to Sonogashira cross-coupling conditions to afford dienyne **66** in an excellent 94% yield (Scheme 12). A stepwise formation of (bis)dienyne **82** was achieved by DCC-mediated coupling of dienyne **66** and carboxylic acid **75** followed by another Sonogashira coupling of the resulting vinyl iodide to enyne **67**. Selective hydrolysis of the methyl ester in the presence of the internal ester linkage using LiOH followed by Yamaguchi macrolactonization led to the advanced intermediate tetradehydrodisorazole C_1 **83**. A direct dimerization of the carboxylic acid derived from hydrolysis of dienyne **66** under high-dilution (0.6 mM) Yamaguchi esterification/ macrolactonization conditions to afford bisdienyne **83** in 59% yield was also reported by Wipf.[26] After extensive optimizations, oxidative cleavage of both PMB ethers of **83** in the presence of DDQ under buffered conditions was found to generate the free bisallylic alcohol in a satisfactory 61% yield. Finally, unmasking of the labile triene unit was realized through a carefully monitored partial reduction of bisalkyne **83** in the presence of Lindlar's catalyst and excess quinoline to complete the first total synthesis of (−)-disorazole in 20 linear steps from known alcohol **68** and in 1.5% overall yield. Synthetic (−)-disorazole C_1 was compared to the analytical data reported for the original sample[1] and was found to be identical in all regards (^{1}H NMR, ^{13}C NMR, HRMS, $[\alpha]_D$). As of late 2008, Wipf's synthesis of (−)-disorazole C_1 remains the only report of a completed synthesis of a member of the disorazole family, fourteen years after their initial discovery.

4.4 Hoffmann's synthesis of a masked northern hemisphere of disorazoles A_1 and D_1

Disorazole A_1 constitutes the largest component of the original 29 macrodiolides isolated from the fermentation broth of *Sorangium cellulosum*.[1] Although disorazole A_1 was found to be too cytotoxic for direct application in anticancer therapy (IC_{50} = 3 pg/mL, cell line L929, mouse fibroblasts, *vide supra*),[12] the mode of action of the disorazoles as well as their structure–activity relationships (SARs) remain an interesting topic for chemists and biologists. The structure of disorazole A_1 is particularly challenging among members of the disorazole family due to the presence of the electrophilic vinyl-dienyl epoxide at C-9/C-10. The synthetic approach of Hoffmann and co-workers involved an esterification/lactonization of southern hemisphere **41** and northern hemisphere **84** (Fig. 9).[40] The synthesis of dienyne fragment **41** was described earlier by Hoffmann (Scheme 6, *vide supra*).[36,38] Vinyl epoxide **84** was derived from phosphonium salt **86** and oxazole **85** *via* a Wittig olefination. The labile (*Z*)-alkenes at C-9′/C-10′ and C-5/C-6 were again masked as alkynes.

Hoffmann's synthesis of northern fragment **84** commenced with a Sharpless dihydroxylation of the known oxazole **87**,[48] followed by oxidative cleavage of the resulting glycol in the presence of $Pb(OAc)_4$ to provide aldehyde **88** in 87% overall yield (Scheme 13). Alternatively, aldehyde **88** was obtained in 68% yield by a one step protocol using $NaIO_4$ on silica gel in the presence of catalytic $RuCl_3$ hydrate. Corey-Fuchs homologation of aldehyde **88** provided alkyne **90** in a disappointing 21% yield. Through brief optimizations, Hoffmann *et al*. found that treatment of aldehyde **88** with Ohira–Bestmann reagent afforded the desired alkyne **90** in a moderately improved yield of 50%. Model studies under a variety of reaction conditions (*e.g.* variations of catalyst, base, solvent, concentration, order of addition, and temperature) revealed that a direct Sonogashira coupling of alkyne **90** to vinyl epoxide test substrate **92** yielded at best 15% of enyne **93**. The authors realized that the sensitive epoxide at C-9/C-10 required a late stage instalment, thereby suggesting a slightly revised synthetic strategy.

As a modified approach, Sonogashira cross-coupling of dibromide **89** to readily available vinyl stannane **94**[40] provided bromotriene **95** in 86% yield. A single step debromination and silyl ether cleavage was accomplished in the presence of excess TBAF to yield allylic alcohol **96** in 87%. Sharpless asymmetric epoxidation of dienyne **96** followed by oxidation of the primary alcohol afforded the desired vinyl epoxy aldehyde **97** in 86% enantiomeric excess. Wittig olefination of aldehyde **97** in the presence of phosphonium salt **86**, prepared in a straightforward manner from the previously synthesized allylic alcohol **50** in 5 steps (Scheme 13),[36] completed the synthesis of the key fragment **84**. As a side note, the TIPS ester at C-16 of alkyliodide **98** was utilized in place of the corresponding MOM and SEM ethers, as described previously in Hoffmann's approach towards disorazole C_1 (*vide supra*), to circumvent stability issues encountered during the halogenation step providing iodide **98**.

In addition to the completion of the masked northern hemisphere **84** of disorazole A_1, Hoffmann successfully synthesized a more stable analog by replacing the vinyl epoxide at C-9/C-10 of disorazole A_1 with a cyclopropane unit (Scheme 14).[41,49] Asymmetric Charette cyclopropanation of mono-PMB protected cis-butene diol **99** followed by Dess–Martin oxidation afforded aldehyde **100**. Subsequent Takai olefination of aldehyde **100** provided vinyl iodide **101** in a moderate 49% yield. Sonogashira cross-coupling of the vinyl iodide with previously prepared alkyne **90** followed by DDQ cleavage of the PMB ether and subsequent Dess–Martin oxidation of the resulting primary alcohol yielded the advanced oxazole **103**. Finally, completion of the masked cyclopropane analog was achieved by a Wittig olefination between aldehyde **103** and the previously prepared alkyl iodide **98** to provide **104** in a 40% yield and ≥5: 1 *Z/E* selectivity. Unfortunately, no biological data on this fragment or any corresponding macrocyclic C-9/C-10 cyclopropane-containing analogs are available.

As an extension of Hoffmann's approach towards the synthesis of a more stable analog of disorazole A_1, the vinyl epoxide at C9/C10 was substituted with an acetonide protected 1,2-diol unit, effectively providing a masked northern fragment of disorazole D_1 (**6**) (Scheme 15).[41] Although the absolute stereochemistry of the 1,2-diol segment of disorazole D_1 has yet to be unambiguously assigned, Hoffmann *et al*. began their synthesis with the C_2-symmetric diol **106** derived from tartaric acid utilizing a protocol reported by Seebach and Hunger-bühler.[50] Mono-protection of diol **106** followed by Parikh–Doering oxidation and Takai olefination provided vinyl iodide **107**. Sonogashira cross-coupling with the previously reported alkyne **90** (Scheme 13, *vide supra*) afforded enyne **108** in 86% yield. Completion of the masked analog **110** was achieved by an initial silyl ether cleavage followed by Dess–Martin oxidation and subsequent Wittig olefination of the resulting aldehyde with phosphonium iodide **86** (*Z/E* = 10: 1).

5 Conclusions

The disorazoles have proven themselves as structurally intriguing, synthetically challenging natural products with impressive *in vitro* anti-cancer activities. The exact binding site of the disorazoles remains uncertain although several biological studies suggest that they bind at or near the vinca domain. The identification of the biosynthetic gene cluster of the disorazoles has opened the possibility for genetic engineering to provide substantial quantities of these metabolites in an expedient manner. Both their complex architecture and labile functionalities present organic chemists with formidable tasks, and only a single total synthesis has been completed in the past fourteen years. Although industries have shifted their focus to small organic molecules of non-natural origin as a primary source for therapeutic drugs, it is without a doubt that the vast amount of information available in the field of natural products will continue to provide an intellectual playground for biologists and synthetic chemists alike. It is eminently feasible that a disorazole or a synthetic compound inspired by the disorazoles will emerge as a therapeutic agent in the not too distant future.[51]

6 Acknowledgments

The authors thank the National Cancer Institute for grant support (CA78039). We also gratefully acknowledge the contributions and stimulating discussions of our collaborators Thomas Graham, Andreas Vogt, Rachel Sikorski, Alexander Ducruet, Fenfeng Yu, Marni Brisson, Carolyn Kitchens, Bethany Petrik, Brianne Raccor, Raghavan Balachandran, Jane Stout, Claire Walczak, Celeste Reese, William Saunders, Billy Day, and, especially, John Lazo.

Biography

Chad Hopkins obtained his B.Sc. (2001) in Chemistry from Mississippi State University. He then moved to the University of Kansas to pursue his Ph.D. under the supervision of Professor Helena Malinakova, where his research was focused on the development of novel palladium-catalyzed multi-component coupling and cascade processes for the synthesis of homoallylic alcohols, amines, δ-lactones, and unnatural amino acids. After completion of his Ph.D. in 2007 he joined the group of Professor Peter Wipf at the University of Pittsburgh as a postdoctoral research associate and is currently working on the synthesis of analogs of the natural product disorazole C_1.

Peter Wipf received his Dipl. Chem. and Ph.D. in Chemistry in 1984 and 1987, respectively, from the University of Zürich under the direction of Prof. Heinz Heimgartner. From 1988 −1990, he was a Swiss National Science Postdoctoral Fellow in the laboratory of Prof. Robert E. Ireland at the University of Virginia. In 1990, he joined the faculty at the University of Pittsburgh, and since 2004 he has been a Distinguished University Professor of Chemistry. At

the center of his research program is natural product synthesis, the study of chemical reactivity and the use of synthesis to augment the chemical toolbox and develop new therapeutic strategies.

7 References

1. Jansen R, Irschik H, Reichenbach H, Wray V, Höfle G. Liebigs Ann. Chem 1994:759–773.
2. Gerth K, Pradella S, Perlova O, Beyer S, Müller R. J. Biotechnol 2003;106:233–253. [PubMed: 14651865]
3. Pronzato P. Drugs 2008;68:139–146. [PubMed: 18197722]Trivedi M, Budihardjo I, Loureiro K, Reid TR, Ma JD. Future Oncol 2008;4:483–500. [PubMed: 18684060]Reichenbach H, Höfle G. Drugs in R&D 2008;9:1–10.Altaha R, Fojo T, Reed E, Abraham J. Curr. Pharm. Des 2002;8:1707–1712. [PubMed: 12171542]
4. Jansen R, Washausen P, Kunze B, Reichenbach H, Höfle G. Eur. J. Org. Chem 1999:1085–1089.Jansen R, Kunze B, Reichenbach H, Höfle G. Liebigs Ann 1996:285–290.Kunze B, Jansen R, Sasse F, Höfle G, Reichenbach H. J. Antibiot 1995;48:1262–1266. [PubMed: 8557566]
5. Jansen R, Kunze B, Reichenbach H, Höfle G. Eur. J. Org. Chem 2000:913–919.Kunze B, Jansen R, Sasse F, Höfle G, Reichenbach H. J. Antibiot 1998;51:1075–1080. [PubMed: 10048565]
6. Sasse F, Steinmetz H, Höfle G, Reichenbach H. J. Antibiot 1995;48:21–25. [PubMed: 7868385]
7. Horstmann N, Menche D. Chem. Commun 2008:5173–5175.Sasse F, Steinmetz H, Höfle G, Reichenbach H. J. Antibiot 1993;46:741–748. [PubMed: 8514628]
8. Sasse F, Steinmetz H, Heil J, Höfle G, Reichenbach H. J. Antibiot 2000;53:879–885. [PubMed: 11099220]
9. Reichenbach H. J. Ind. Microbiol. Biotech 2001;27:149–156.
10. Kopp M, Irschik H, Pradella S, Müller R. ChemBioChem 2005;6:1277–1286. [PubMed: 15892181]
11. Carvalho R, Reid R, Viswanathan N, Gramajo H, Julien B. Gene 2005;359:91–98. [PubMed: 16084035]
12. Irschik H, Jansen R, Gerth K, Höfle G, Reichenbach H. J. Antibiot 1995;48:31–35. [PubMed: 7868386]
13. Hearn BR, Arslanian RL, Fu H, Liu F, Gramajo H, Myles DC. J. Nat. Prod 2006;69:148–150. [PubMed: 16441089]
14. Elnakady YA, Sasse F, Lünsdorf H, Reichenbach H. Biochem. Pharmacol 2004;67:927–935. [PubMed: 15104246]
15. For a review on the function of tubulin and role of antitubulin drugs, see: Pellegrini F, Budman DR. Cancer Invest 2005;23:264–273.273 [PubMed: 15948296]
16. Cruz-Monserrate Z, Mullaney JT, Harran PG, Pettit GR, Hamel E. Eur. J. Biochem 2003;270:3822–3828. [PubMed: 12950266]
17. Khalil MW, Sasse F, Lünsdorf H, Elnakady YA, Reichenbach H. ChemBioChem 2006;7:678–683. [PubMed: 16491500]
18. Wipf P, Reeves JT, Day BW. Curr. Pharm. Des 2004;10:1417–1437. [PubMed: 15134491]and references cited therein
19. Schiff PB, Fant J, Horowitz SB. Nature 1979;277:665–667. [PubMed: 423966]
20. Bollag DM, McQueney PA, Zhu J, Hensens O, Koupal L, Liesch J, Goetz M, Lazarides E, Woods CM. Cancer Res 1995;55:2325–2333. [PubMed: 7757983]
21. ter Haar E, Kowalski RJ, Hamel E, Lin CM, Longley RE, Gunasekera SP, Rosenkranz HS, Day BW. Biochemistry 1996;35:243–250. [PubMed: 8555181]
22. Madiraju C, Edler MC, Hamel E, Raccor BS, Van Balachandran R, Zhu G, Guiliano KA, Vogt A, Shin Y, Fournier J-H, Fukui Y, Brueckner AM, Curran DP, Day BW. Biochemistry 2005;44:15053–15063. [PubMed: 16274252]
23. Mooberry SL, Tien G, Hernandez AH, Plubrukarn A, Davidson BS. Cancer Res 1999;59:653–660. [PubMed: 9973214]
24. Gallagher BM Jr. Curr. Med. Chem 2007;14:2959–2967. [PubMed: 18220732]Altmann K-H, Gertsch J. Nat. Prod. Rep 2007;24:327–357. [PubMed: 17390000]

25. Ross DD. Leukemia 2000;14:467–473. [PubMed: 10720143]Hsia T-C, Lin C-C, Wang J-J, Ho S-T, Kao A. Lung 2002;180:173–179. [PubMed: 12177731]Lehne G. Curr. Drug Targets 2000;1:85–99. [PubMed: 11475537]Dumontet C, Sikic BI. J. Clin. Oncol 1999;17:1061–1070. [PubMed: 10071301]Gottesman MM, Fojo T, Bates SE. Nat. Rev. Cancer 2002;2:48–58. [PubMed: 11902585]
26. Wipf P, Graham TH, Xiao J. Pure Appl. Chem 2007;79:753–761.
27. Wipf P, Graham TH, Vogt A, Silkorski RP, Ducruet AP, Lazo JS. Chem. Biol. Drug Des 2006;67:66–73. [PubMed: 16492150]
28. Tierno MB, Kitchens CA, Petrik B, Graham TH, Wipf P, Xu F, Saunders W, Raccor BS, Balachandran R, Day BW, Stout JR, Walczak CE, Ducruet AP, Reese CE, Lazo JS. J. Pharmacol. Exp. Ther 2009;328:715–722. [PubMed: 19066338]
29. Hillier MC, Park DH, Price AT, Ng R, Meyers AI. Tetrahedron Lett 2000;41:2821–2824.
30. Phillips AJ, Uto Y, Wipf P, Reno MJ, Williams DR. Org. Lett 2000;2:1165–1168. [PubMed: 10804580]
31. Stork G, Zhao K. Tetrahedron Lett 1989;30:2173–2174.
32. Kiyooka S, Kaneko Y, Komura M, Matsuo H, Nakano M. J. Org. Chem 1991;56:2276–2278.
33. Hillier MC, Price AT, Meyers AI. J. Org. Chem 2001;66:6037–6045. [PubMed: 11529729]
34. Kira, M.; Iwamoto, T. Chemistry of Organic Silicon Compounds. Rappoport. Apeloig, ZY., editor. Vol. 3. John Wiley & Sons Ltd.; Chichester: 2001. p. 853-948.Hillier MC, Meyers AI. Tetrahedron Lett 2001;42:5145–5147.
35. Höfle, G. GBF Annual Report. 19992000.
36. Hartung IV, Niess B, Haustedt LO, Hoffmann HMR. Org. Lett 2002;4:3239–3242. [PubMed: 12227758]
37. Keck GE, Krishnamurthy D. Org. Synth 1998;75:12–18.
38. Niess B, Hartung IV, Haustedt LO, Hoffmann HMR. Eur. J. Org. Chem 2006:1132–1143.
39. Wipf P, Graham TH. J. Am. Chem. Soc 2004;126:15346–15347. [PubMed: 15563138]
40. Hartung IV, Eggert U, Haustedt LO, Niess B, Schäfer PM, Hoffmann HMR. Synthesis 2003:1844–1850.
41. Haustedt LO, Panicker SB, Kleinert M, Hartung IV, Eggert U, Niess B, Hoffmann HMR. Tetrahedron 2003;59:6967–6977.
42. Bode JW, Gauthier DR, Carreira EM. Chem. Commun 2001:2560–2561.
43. Gao G, Moore D, Xie R-G, Pu L. Org. Lett 2002;4:4143–4146. [PubMed: 12423107]
44. Marshall JA, Bourbeau MP. Org. Lett 2003;5:3197–3199. [PubMed: 12943386]
45. Zhao M, Li J, Mano E, Song Z, Tschaen DM, Grabowski EJJ, Reider PJ. J. Org. Chem 1999;64:2564–2566.
46. Vakalopoulos A, Smits R, Hoffmann HMR. Eur. J. Org. Chem 2002:1538–1545.
47. Corey EJ, Rucker C. Tetrahedron Lett 1982;23:719–722.
48. Panek JS, Beresis RT. J. Org. Chem 1996;61:6496–6497. [PubMed: 11667510]
49. For examples involving the substitution of an epoxide with a cyclopropane unit in the epothilone and radicicol series, see: Kuzniewski CN, Gertsch J, Wartmann M, Altmann K-H. Org. Lett 2008;10:1183–1186.1186 [PubMed: 18303900];Nicolaou KC, Sasmal PK, Rassias G, Reddy MV, Altmann K-H, Wartmann M, O'Brate A, Giannakakou P. Angew. Chem., Int. Ed 2003;42:3515–3520.3520;Nicolaou KC, Ritzén A, Namoto K, Buey RM, Díaz JF, Andreu JM, Wartmann M, Altmann K-H, O'Brate A, Paraskevi G. Tetrahedron 2002;58:6413–6432.6432;Nicolaou KC, Namoto K, Li J, Ritzén A, Ulven T, Shoji M, Zaharevitz D, Gussio R, Sackett DL, Ward RD, Hensler A, Fojo T, Giannakakou P. ChemBioChem 2001;2:69–75.75 [PubMed: 11828429];Yang Z-Q, Geng X, Solit D, Pratilas CA, Rosen N, Danishefsky SJ. J. Am. Chem. Soc 2004;126:7881–7889.7889 [PubMed: 15212536];Yamamoto K, Garbaccio RM, Stachel SJ, Solit DB, Chiosis G, Rosen N, Danishefsky SJ. Angew. Chem., Int. Ed 2003;42:1280–1284.1284
50. Hungerbühler E, Seebach D. Helv. Chim. Acta 1981;64:687–702.
51. Newman DJ, Cragg GM. J. Nat. Prod 2004;67:1216–1238. [PubMed: 15332835]

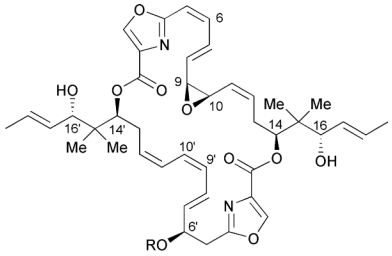

Disorazole A_1 (**1**) 69.8%, (R = Me)
Disorazole A_2 (**2**) 0.9%, (R = H)
Disorazole A_4 (**3**) 2.1%, (R = Me, 11' *E*)
Disorazole A_5 (**4**) 2.7%, (R = Me, 9',11' *E*)
Disorazole A_7 (**5**) 1.6%, (R = Me, *trans*-epoxide)
Disorazole D_1 (**6**) 1.4%, (R = Me, 9',10' diol)

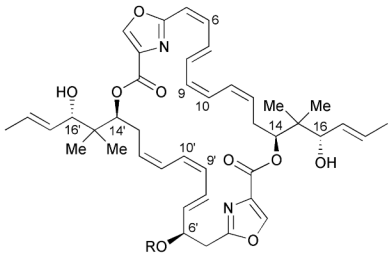

Disorazole F_1 (**7**) 3.7%, (R = Me)
Disorazole F_2 (**8**) 0.5%, (R = H)
Disorazole F_3 (**9**) 0.4%, (R = Me, 9,11 *E*)

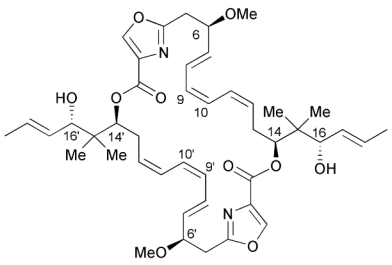

Disorazole C_1 (**10**) 0.3%

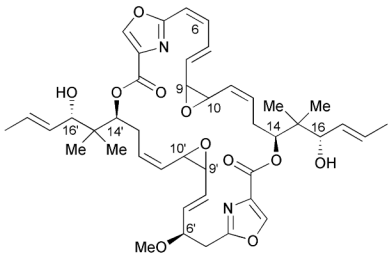

Disorazole E_1 (**11**) 8.7%
Disorazole E_2 (**12**) <0.1%, (*trans*-9,10-epoxide)
Disorazole E_3 (**13**) 0.1%, ((7*Z*)-*trans*-9,10-epoxide)

Fig. 1.
Selected members of the disorazole family. Percentages correspond to relative amounts isolated from So ce12.

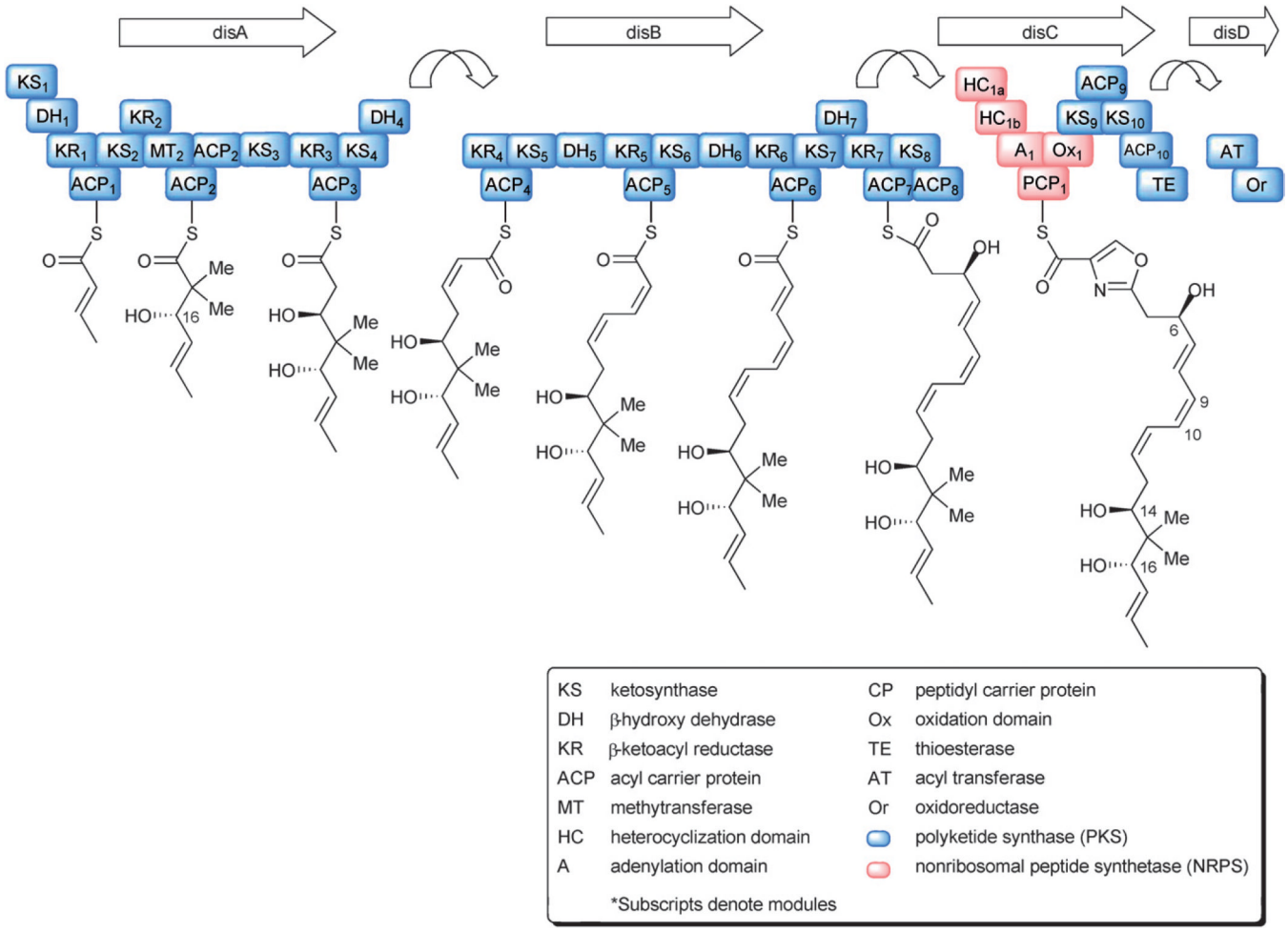

Fig. 2.
Proposed biosynthetic pathway for the disorazoles.

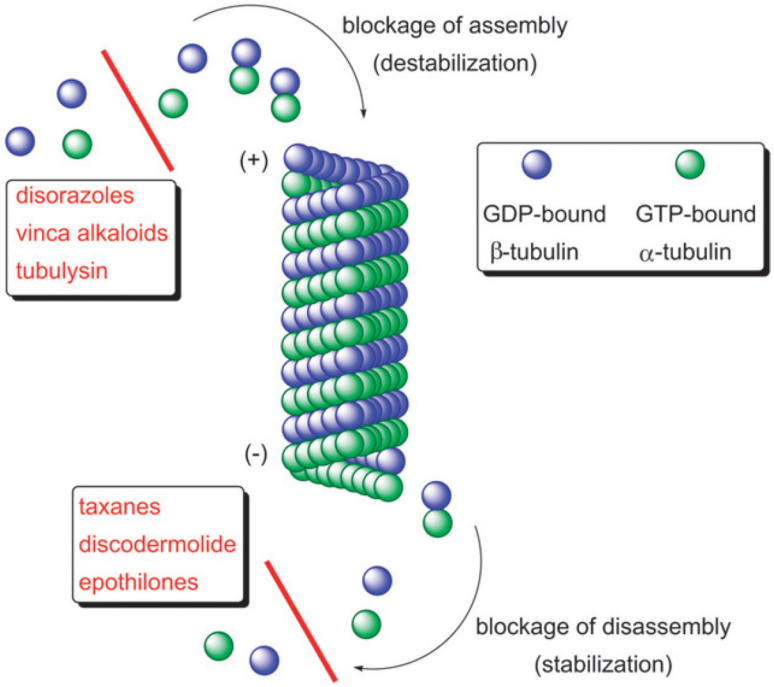

Fig. 3.
Stabilization and destabilization of microtubule formation by anti-cancer agents.

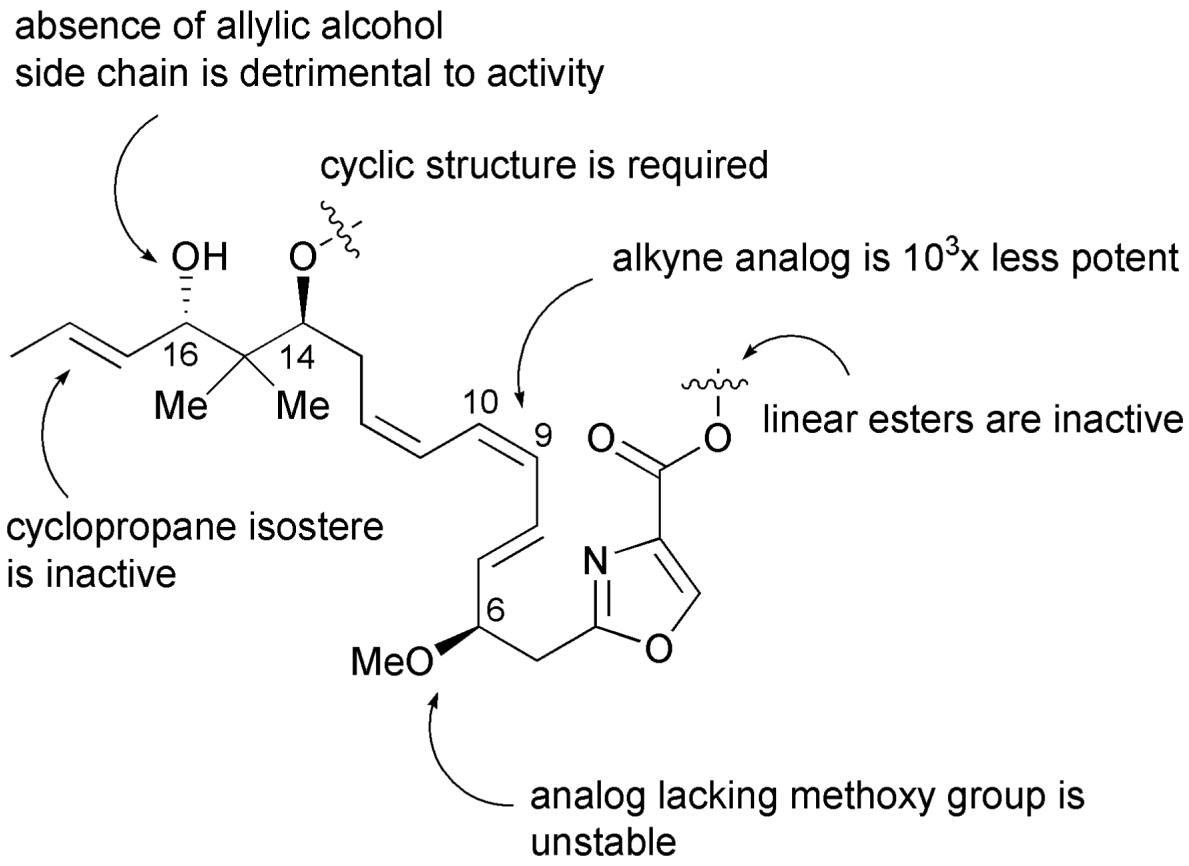

Fig. 4.
Summary of disorazole C_1 (**10**) SAR studies.

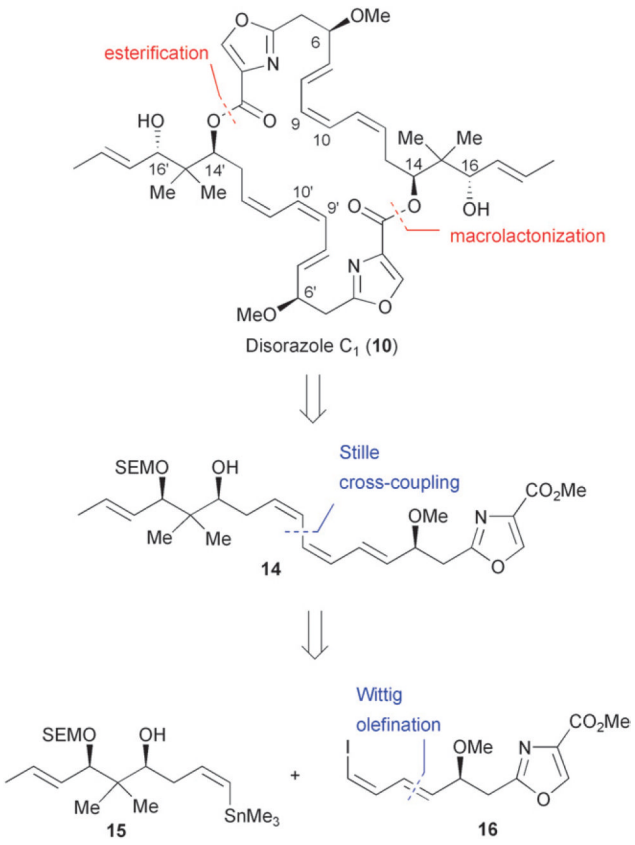

Fig. 5.
Meyers' retrosynthetic analysis of disorazole C_1 (**10**).

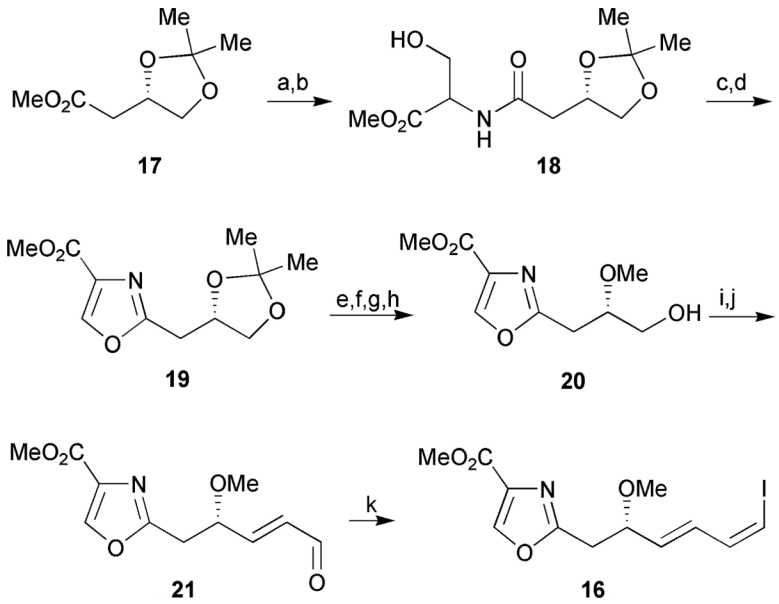

Scheme 1.

Meyers' oxazole segment synthesis. *Reagents and conditions*: (a) 2N LiOH, THF; (b) D,L-Ser·OMe, 1,1′-CDI, THF, 67% (over 2 steps); (c) DAST, CH_2Cl_2, −78 °C; (d) DBU, $BrCCl_3$, 0 °C to rt, 79% (over 2 steps); (e) Dowex-H^+, MeOH; (f) TIPSOTf, 2,6-lutidine, CH_2Cl_2 (0.05M), −78 °C, 74% (over 2 steps); (g) MeI, Ag_2O, CH_3CN, Δ; (h) TBAF, THF, 75% (over 2 steps); (i) SO_3·Pyr, DMSO, Et_3N, CH_2Cl_2; (j) $Ph_3P{=}CH_2CHO$, benzene, Δ, 62% (over 2 steps); (k) $I^-Ph_3P^+CH_2I$, NaHMDS, HMPA, THF, −78 °C, 71%.

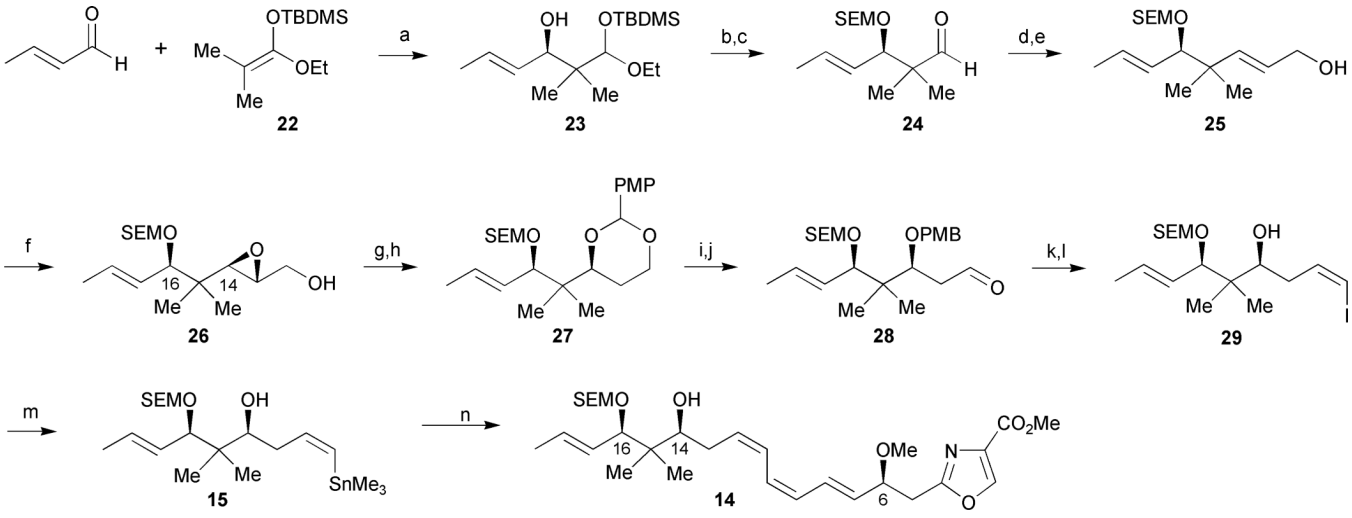

Scheme 2.

Meyers' 1st generation synthesis of the southern fragment of disorazole C_1. *Reagents and conditions*: (a) BH_3·THF, *N*-Ts-L-Val, CH_2Cl_2, −78 °C, 73%; (b) SEMCl, Hünig's base, CH_2Cl_2, −78 °C; (c) 80% AcOH, 79% (over 2 steps); (d) $(EtO)_2P(O)CH_2CO_2Et$, NaH, toluene/THF, 95%; (e) DIBAL-H, CH_2Cl_2, −78 °C, 76%; (f) D-(−)-DIPT, *t*-BuOOH, $Ti(Oi\text{-}Pr)_4$, CH_2Cl_2, −30 °C, 95%; (g) Red-Al, THF, −20 °C: (h) *p*-methoxybenzylidene dimethyl acetal, PPTS, CH_2Cl_2, 83% (over 2 steps); (i) DIBAL-H, CH_2Cl_2, −78 °C, 92%; (j) Dess–Martin periodinane, pyridine, *t*-BuOH, CH_2Cl_2, 83%; (k) $I^-Ph_3P^+CH_2I$, NaHMDS, HMPA, THF, −78 °C, 67%; (l) DDQ, CH_2Cl_2, H_2O, 79%; (m) $PdCl_2(PPh_3)_2$, $(Me_3Sn)_2$, Li_2CO_3, THF, 74%; (n) $PdCl_2(CH_3CN)_2$, **16**, DMF, 76%.

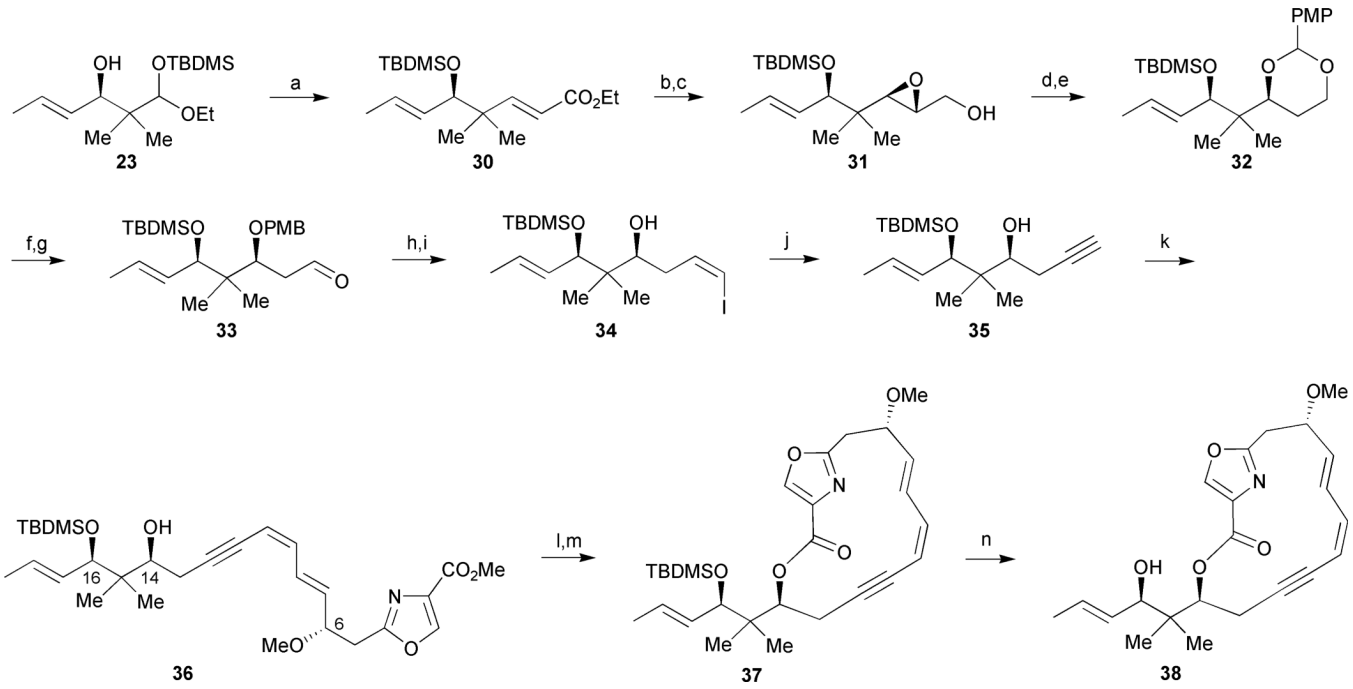

Scheme 3.

Meyers' 2nd generation approach. *Reagents and conditions*: (a) $(EtO)_2P(O)CH_2CO_2Et$, NaH (2.0 equiv), THF, −78 °C to rt, 72%; (b) DIBAL-H, CH_2Cl_2, −78 °C; (c) D-(−)-DIPT, *t*-BuOOH, $Ti(Oi\text{-}Pr)_4$, CH_2Cl_2, −30 °C, 80% (over 2 steps); (d) Red-Al, THF, −20 °C to 0 °C; (e) *p*-methoxybenzylidene dimethyl acetal, PPTS, CH_2Cl_2, 77% (over 2 steps); (f) DIBAL-H, CH_2Cl_2, −78 °C; (g) Dess–Martin periodinane, pyridine, *t*-BuOH, CH_2Cl_2, 90% (over 2 steps); (h) $I^-Ph_3P^+CH_2I$, NaHMDS, HMPA, THF, −78 °C; (i) DDQ, CH_2Cl_2, H_2O, 67% (over 2 steps); (j) NaHMDS (2.0 equiv), THF, −78 °C to rt, 93%; (k) **16**, $PdCl_2(PPh_3)_2$, CuI, Et_3N, CH_3CN, −20 °C to rt, 87%; (l) 1N LiOH, THF; (m) DPTC, DMAP, toluene, Δ, 46% (over 2 steps); (n) HF·Pyr, CH_3CN, 45%.

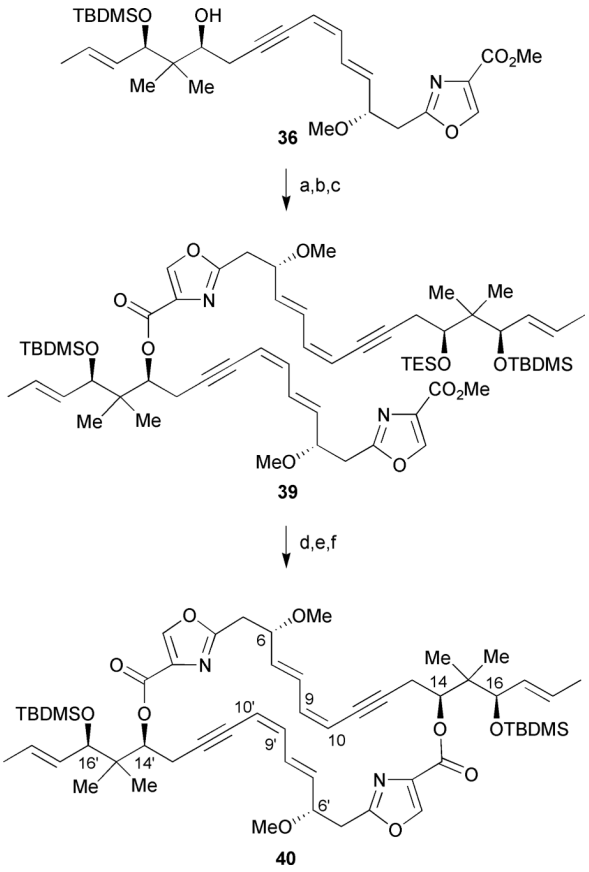

Scheme 4.

Meyers' dimerization approach. *Reagents and conditions*: (a) TESOTF, 2,6-lutidine, CH_2Cl_2, −78 °C, 69%; (b) 1N LiOH, THF; (c) **36**, DPTC, DMAP, toluene, Δ, 65% (over 2 steps); (d) TFA, H_2O, THF, 65%; (e) 1N LiOH, THF; (f) 2,4,6-trichlorobenzoyl chloride, DMAP, toluene, 24% (over 2 steps).

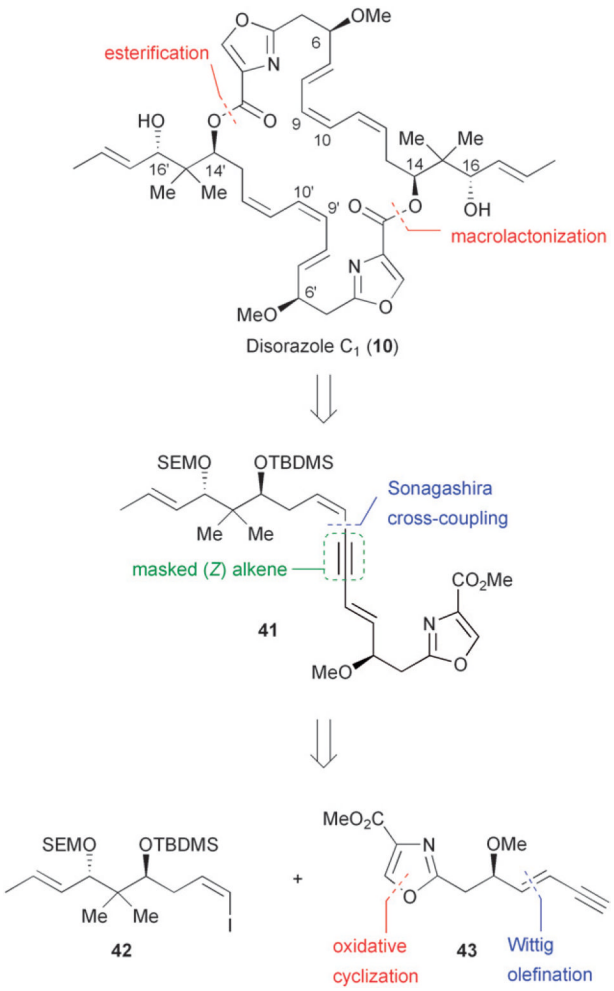

Fig. 6.
Hoffmann's retrosynthetic analysis of disorazole C_1 (**10**).

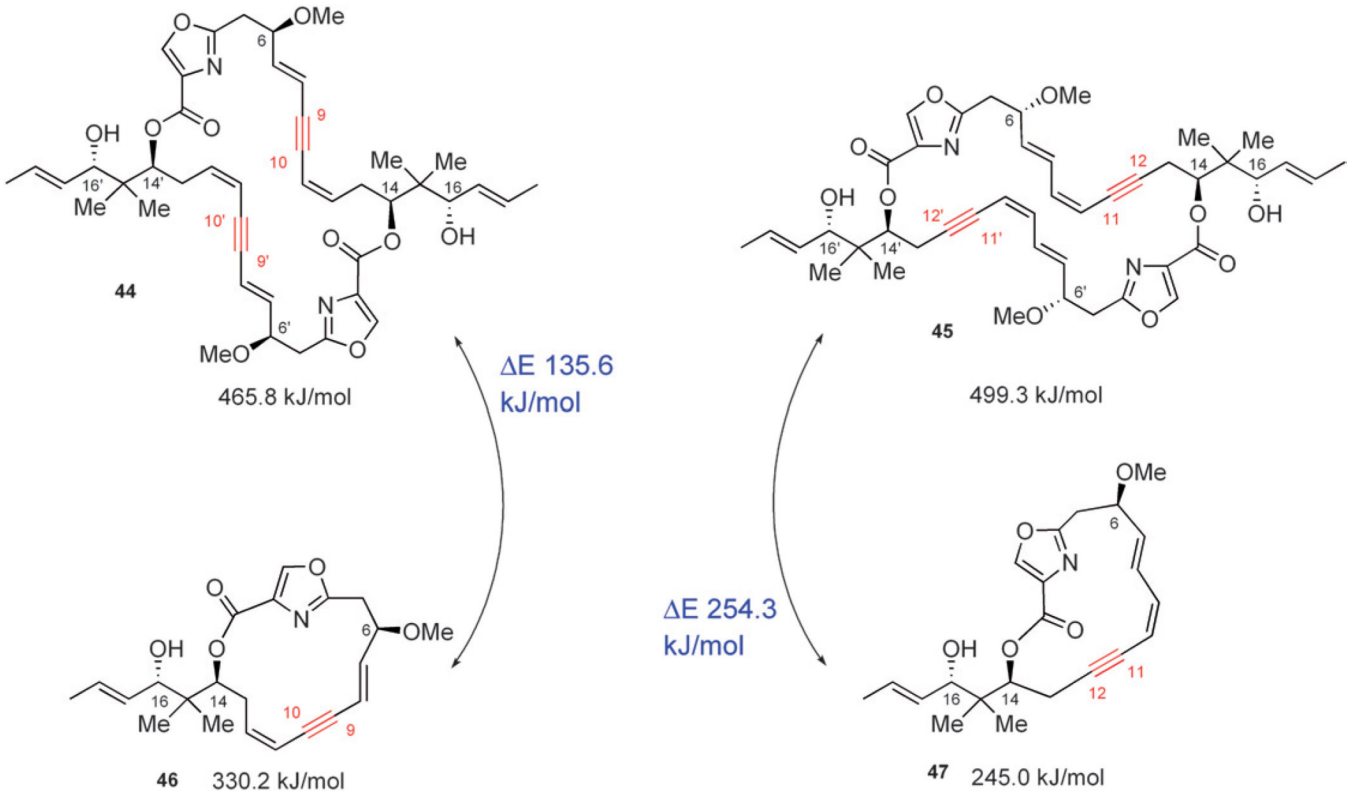

Fig. 7.
Hoffmann's estimates of ring strain of 15- versus 30-membered lactones based on molecular mechanics energy minimizations.

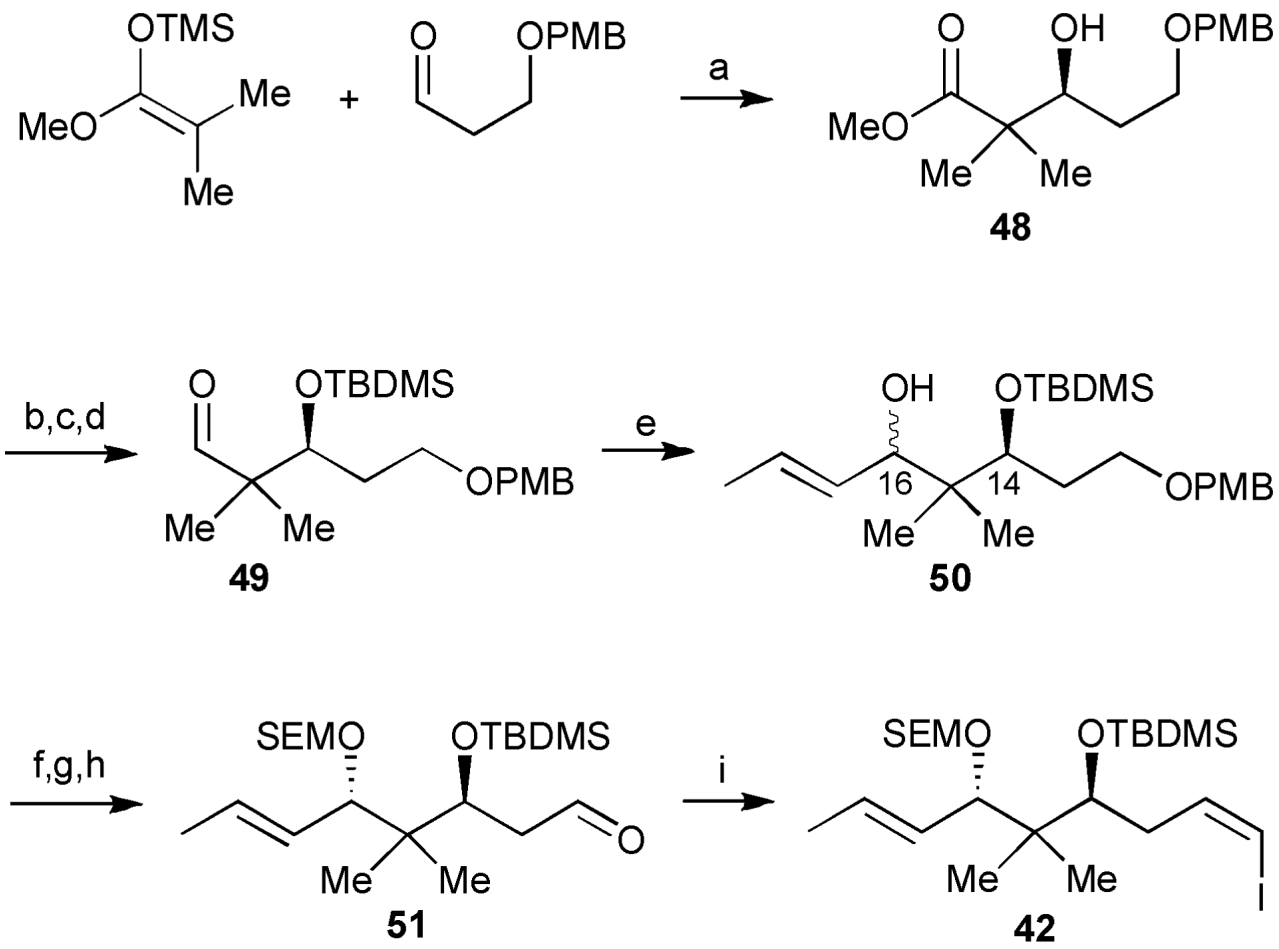

Scheme 5.

Hoffmann's 1st generation C-11 to C-19 segment synthesis. *Reagents and conditions*: (a) BH_3·THF, *N*-Ts-D-Val, CH_2Cl_2, −78 °C, then K_2CO_3, MeOH, 96%; (b) TBDMSOTf, 2,6-lutidine, DMAP, CH_2Cl_2, 99%; (c) DIBAL-H, toluene, −78 °C, 94%; (d) Dess–Martin periodinane, CH_2Cl_2, 0 °C to rt, 83%; (e) *trans*-1-bromopropene, *t*-BuLi, Et_2O/THF, −95 °C, 99% (combined yield of both diastereomers); (f) SEMCl, Hünig's base, Bu_4NI, CH_2Cl_2; (g) DDQ, CH_2Cl_2/H_2O, 0 °C, 98% (yield over 2 steps, based on the (5*S*)-diastereomer of **50**); (h) SO_3·Pyr, Et_3N, CH_2Cl /DMSO, 0 °C, 80%; (i) $I^-Ph_3P^+CH_2I$, NaHMDS, HMPA, THF, −78 °C, 82%.

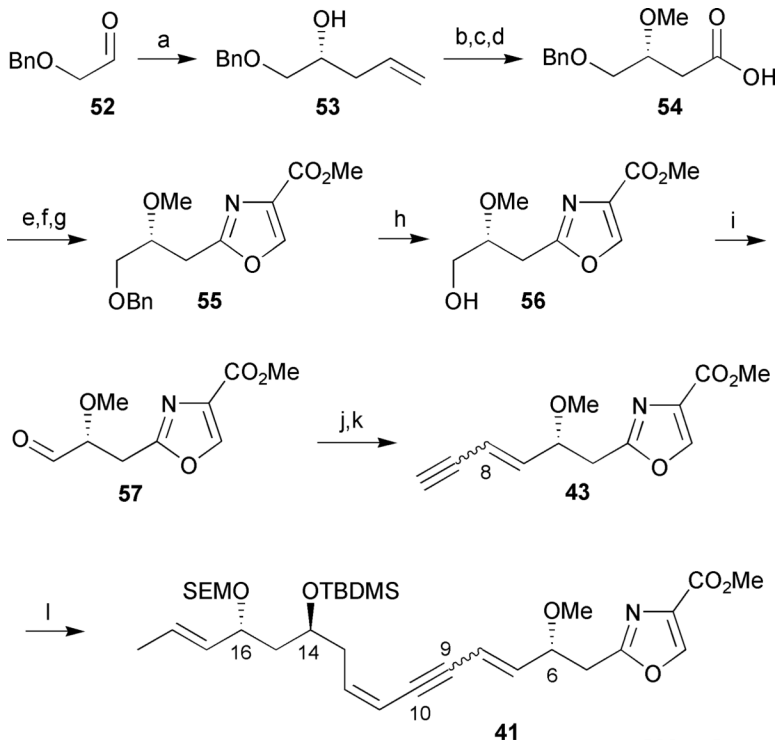

Scheme 6.

Hoffmann's 1st generation synthesis of a masked triene monomer of disorazole C_1. *Reagents and conditions*: (a) (*R*)-BINOL, Ti(O*i*-Pr)$_4$, 4Å MS, allyltributylstannane, CH_2Cl_2, −20 °C, 84%; (b) NaH, MeI, THF, 94%; (c) O_3/O_2, CH_2Cl_2, −78 °C, then PPh_3, −78 °C to rt, 86%; (d) $NaClO_2$, KH_2PO_4, H_2O_2, CH_3CN/MeOH/H_2O, 10 °C, 98%; (e) L-SerOMe·HCl, IBCF, NMM, THF, −25 °C to rt, 71%; (f) DAST, K_2CO_3, CH_2Cl_2, −78 °C; (g) DBU, $BrCCl_3$, CH_2Cl_2, 0 °C to rt, 79% (over 2 steps); (h) H_2, Pd/C, EtOH, 97%; (i) SO_3·Pyr, Et_3N, CH_2Cl_2/DMSO, 0 °C, 75%; (j) $Br^-Ph_3P^+CH_2C{\equiv}CTMS$, *n*-BuLi, THF, −78 °C to 0 °C, 49%; (k) K_2CO_3, MeOH, 77%; (l) **42**, $PdCl_2(PPh_3)_2$, CuI, Et_3N, CH_3CN, −20 °C to rt, 58%.

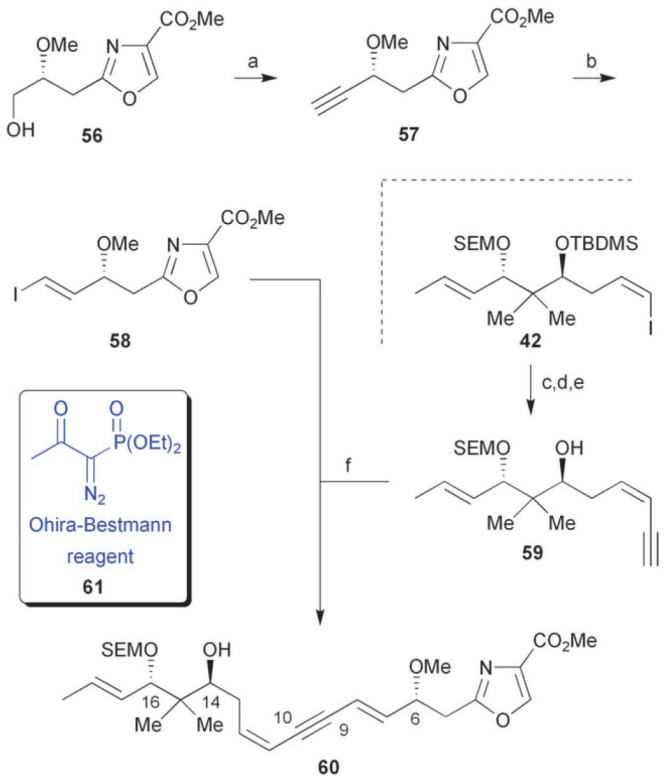

Scheme 7.

Hoffmann's 2nd generation synthesis of a masked triene monomer of disorazole C_1. *Reagents and conditions*: (a) $(ClCO)_2$, Et_3N, DMSO/CH_2Cl_2, −78 °C to −40 °C, then **56**, K_2CO_3, MeOH, 0 °C to rt, 75% (over 2 steps); (b) *n*-Bu_3SnH, $Pd(PPh_3)_4$, THF, then I_2, 88%; (c) TMS-acetylene, $PdCl_2(PPh_3)_2$, CuI, Et_3N, CH_3CN, 99%; (d) TBAF (1.1 equiv), THF, 0 °C to rt, 81%; (e) TBAF (10.0 equiv), THF, 95%; (f) $PdCl_2(PPh_3)_2$, CuI, Et_3N, DMF, 89%.

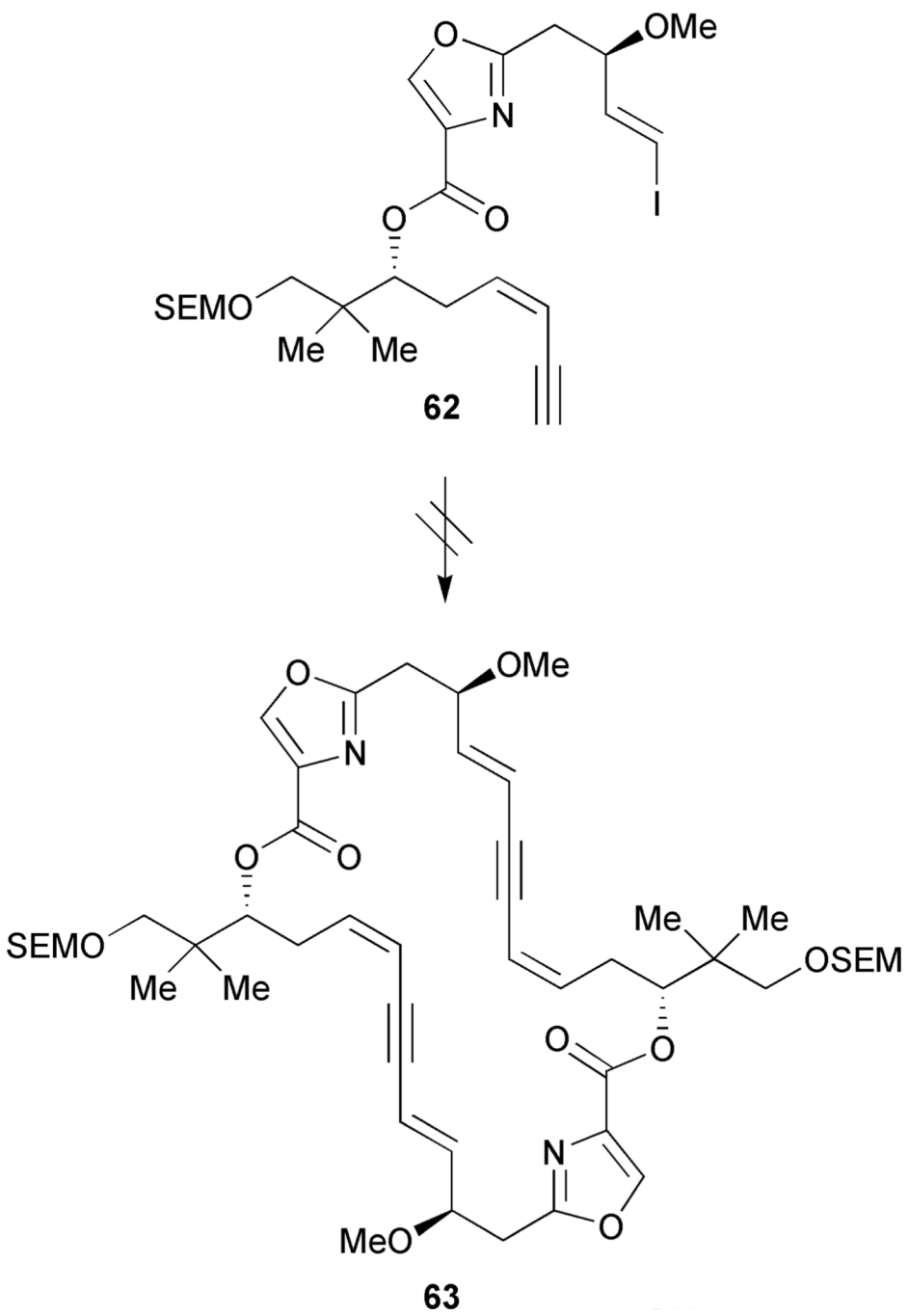

Scheme 8.

Hoffmann's alternative Sonogashira cyclodimerization attempt. *Reagents and conditions*: $PdCl_2(PPh_3)_2$, CuI, Et_3N, DMF, or slow addition of **62** to $PdCl_2(PPh_3)_2$, CuI, Et_3N, THF.

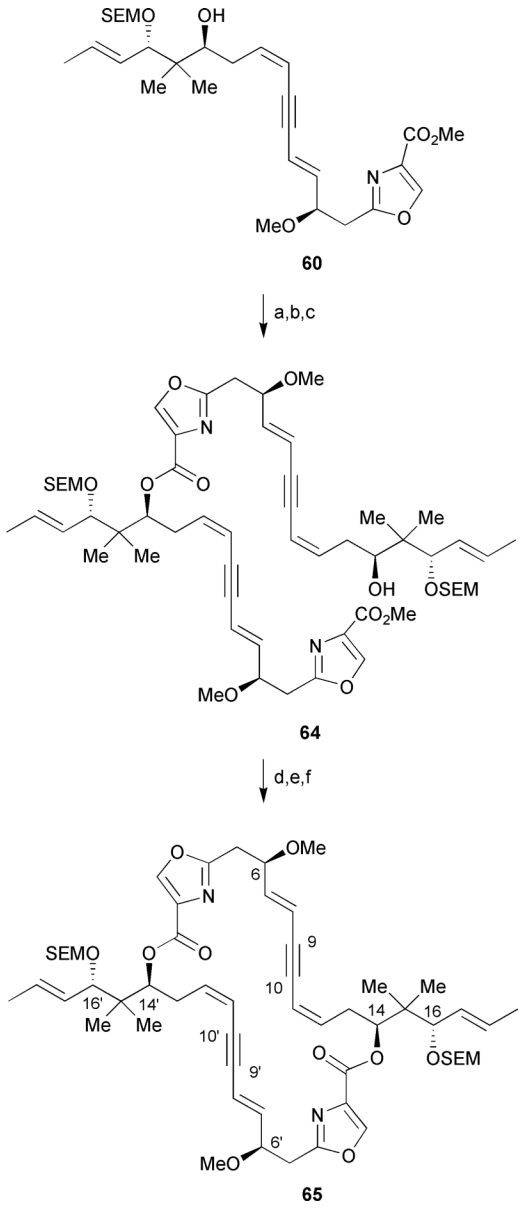

Scheme 9.

Hoffmann's synthesis of tetradehydrodisorazole C_1. *Reagents and conditions*: (a) TESOTf, 2,6-lutidine, DMAP, CH_2Cl_2, −40 °C to −20 °C, 85%; (b) 1N LiOH, H_2O/THF, quant.; (c) 2,4,6-trichlorobenzoyl chloride, Et_3N, toluene, then **60**, DMAP, toluene, 40 °C, 69%; (d) TBAF, AcOH, H_2O/THF, 87%; (e) $Ba(OH)_2$, H_2O/MeOH/THF, quant.; (f) 2,4,6-trichlorobenzoyl chloride, Et_3N, toluene, 40 °C, 31%.

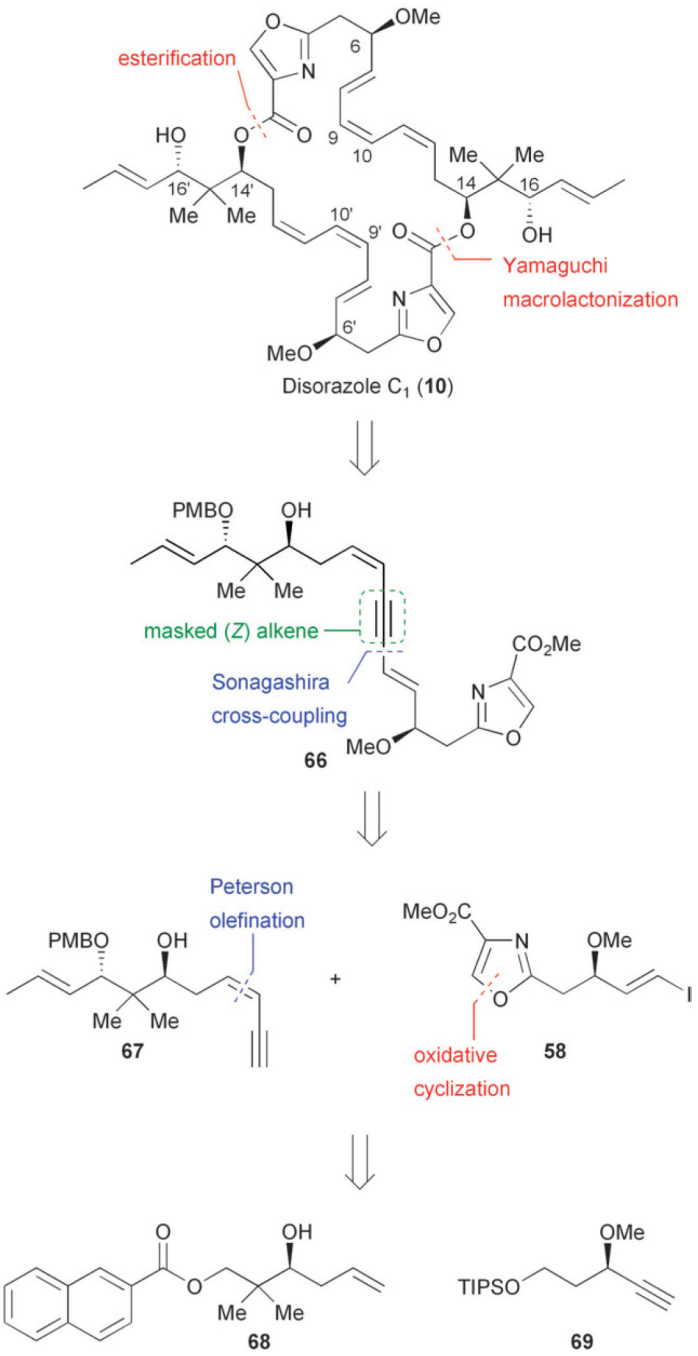

Fig. 8.
Wipf's retrosynthetic analysis of (−)-disorazole C_1 (**10**).

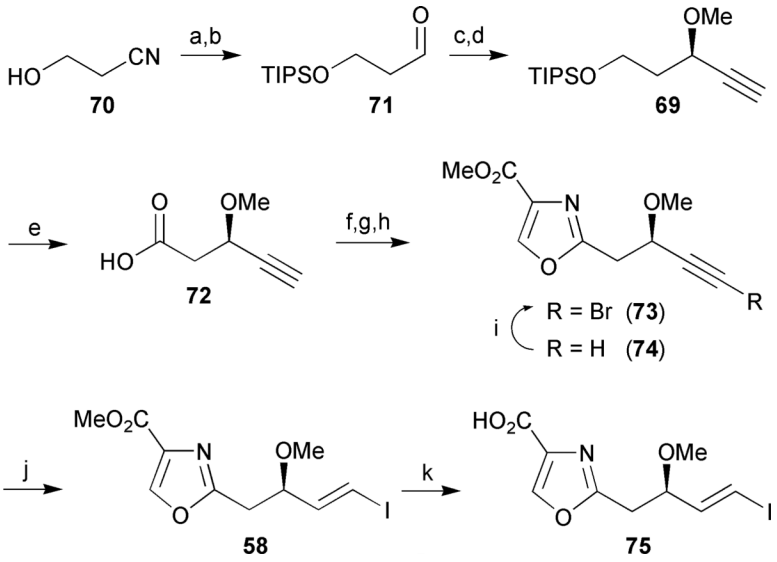

Scheme 10.

Wipf's oxazole segment synthesis. *Reagents and conditions*: (a) TIPSCl, imidazole, DMF; (b) DIBAL-H, CH_2Cl_2, −10 °C, 78% (over 2 steps); (c) TMS-acetylene, Et_2Zn, toluene, Δ, then (*S*)-BINOL, Ti(O*i*-Pr)$_4$, **71**, rt, 66%; (d) dimethyl sulphate, *n*-Bu_4NHSO_4, NaOH, toluene/H_2O, 0 °C to rt, 95%; (e) HF, CH_3CN, then NaOCl, $NaClO_2$, TEMPO, CH_3CN, phosphate buffer (pH 6.7), 45 °C, 99%; (f) SerOMe·HCl, EDC, HOBt, NMM, CH_2Cl_2, 0 °C to rt, 55%; (g) DAST, CH_2Cl_2, then K_2CO_3, −78 °C to rt; (h) DBU, $BrCCl_3$, CH_2Cl_2, 0 °C to 4 °C; (i) NBS, $AgNO_3$, acetone, 54%; (j) *n*-Bu_3SnH, $PdCl_2(PPh_3)$, THF, −78 °C to rt, then I_2, 0 °C, 92%; (k) 1N LiOH, H_2O/THF, 97%.

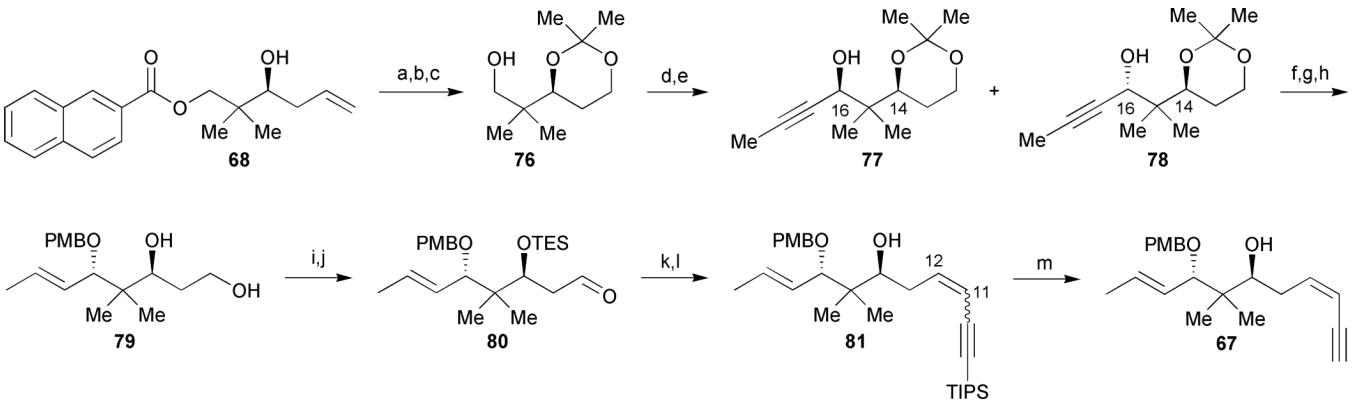

Scheme 11.

Wipf's enyne segment synthesis. *Reagents and conditions*: (a) O_3/O_2, Sudan III, MeOH/CH_2Cl_2, −78 °C, then $NaBH_4$, −78 °C to rt, 88%; (b) 2,2-dimethoxypropane, PPTS, THF, 0 °C to rt, 97%; (c) 1N LiOH, THF/MeOH, 0 °C to rt, 82%; (d) oxalyl chloride, DMSO, Et_3N, −78 °C; (e) propyne, *n*-BuLi, THF, −78 °C to 0 °C; (f) Red-Al, THF (degassed), Δ, 83%; (g) PMBBr, Et_3N, KHMDS, THF, −78 °C to rt; (h) AcOH/THF/H_2O (4:1:1), 60 °C, 84% (over 2 steps); (i) TESOTf, 2,6-lutidine, CH_2Cl_2, 0 °C; (j) oxalyl chloride, DMSO, Et_3N, CH_2Cl_2, −78 °C, 75% (over 2 steps); (k) 1,3-bis(TIPS) propyne, *n*-BuLi, THF, −78 °C; (l) chloroacetic acid, MeOH/CH_2Cl_2; (m) TBAF, THF, 0 °C to rt, 94%.

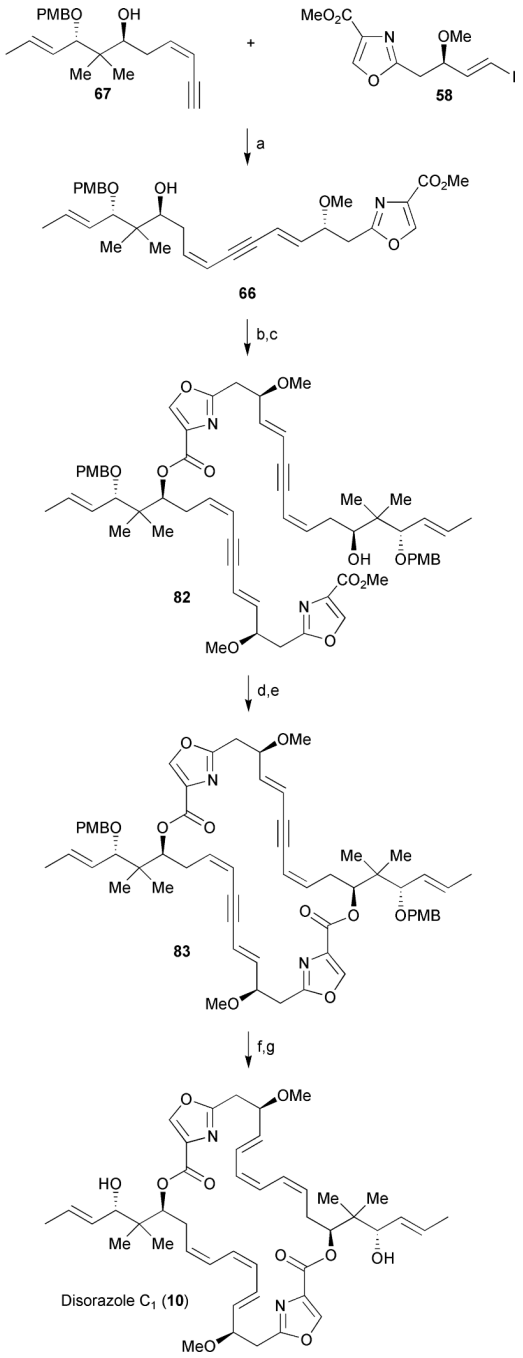

Scheme 12.

Wipf's end game strategy for disorazole C_1. *Reagents and conditions*: (a) $PdCl_2(PPh_3)$, CuI, Et_3N, CH_3CN, −20 °C to rt, 94%; (b) **75**, DCC, DMAP, CH_2Cl_2, 0 °C to rt, 80%; (c) **67**, $PdCl_2(PPh_3)_2$, CuI, Et_3N, CH_3CN, −20 °C to rt, 94%; (d) 1N LiOH, H_2O/THF, 98%; (e) 2,4,6-trichlorobenzoyl chloride, Et_3N, THF, then DMAP, toluene, 79%; (f) DDQ, phosphate buffer (pH 6.7), CH_2Cl_2, 61%; (g) H_2, Lindlar's catalyst, quinoline, EtOAc, 57%.

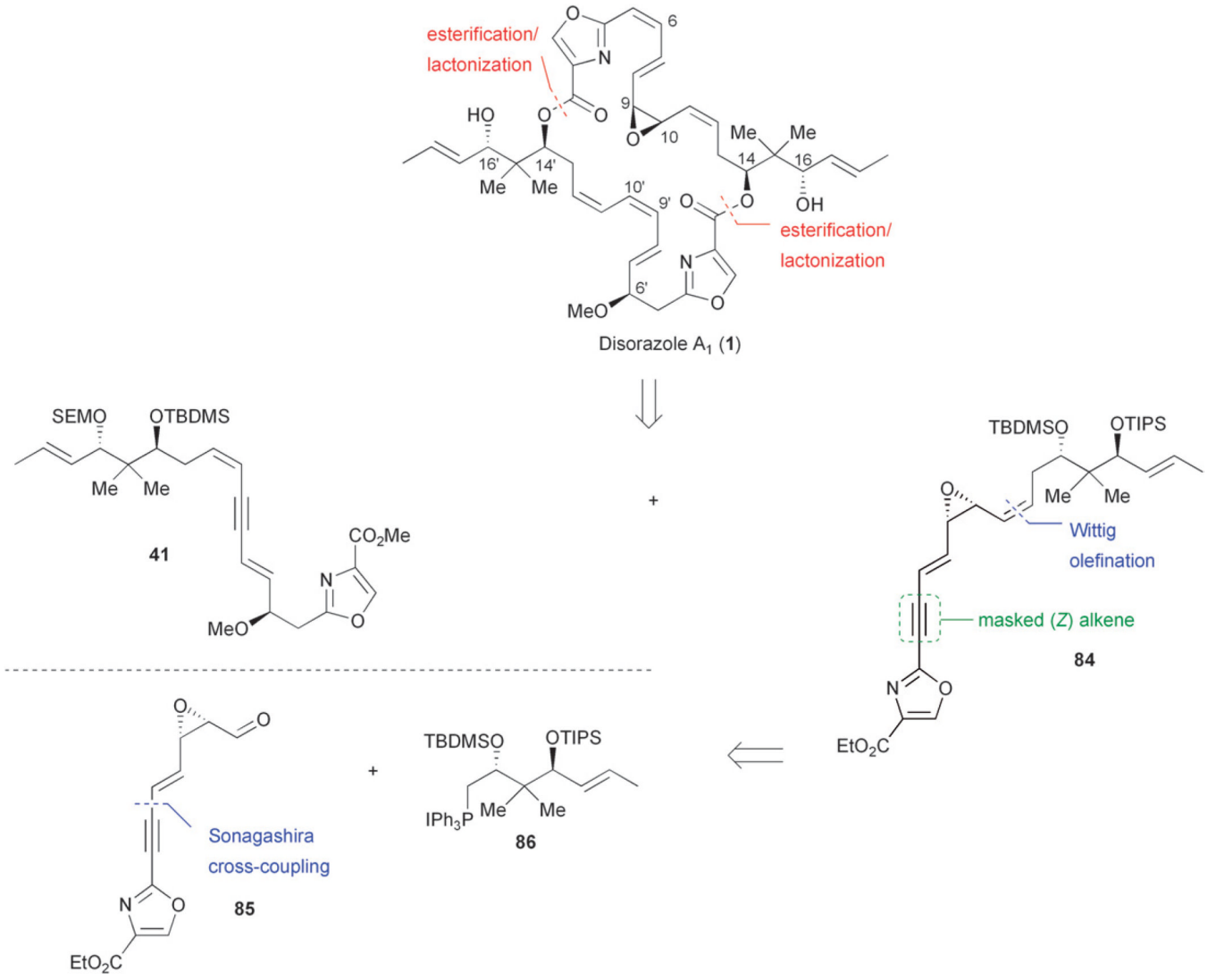

Fig. 9.
Hoffmann's retrosynthetic analysis of disorazole A_1 (**1**).

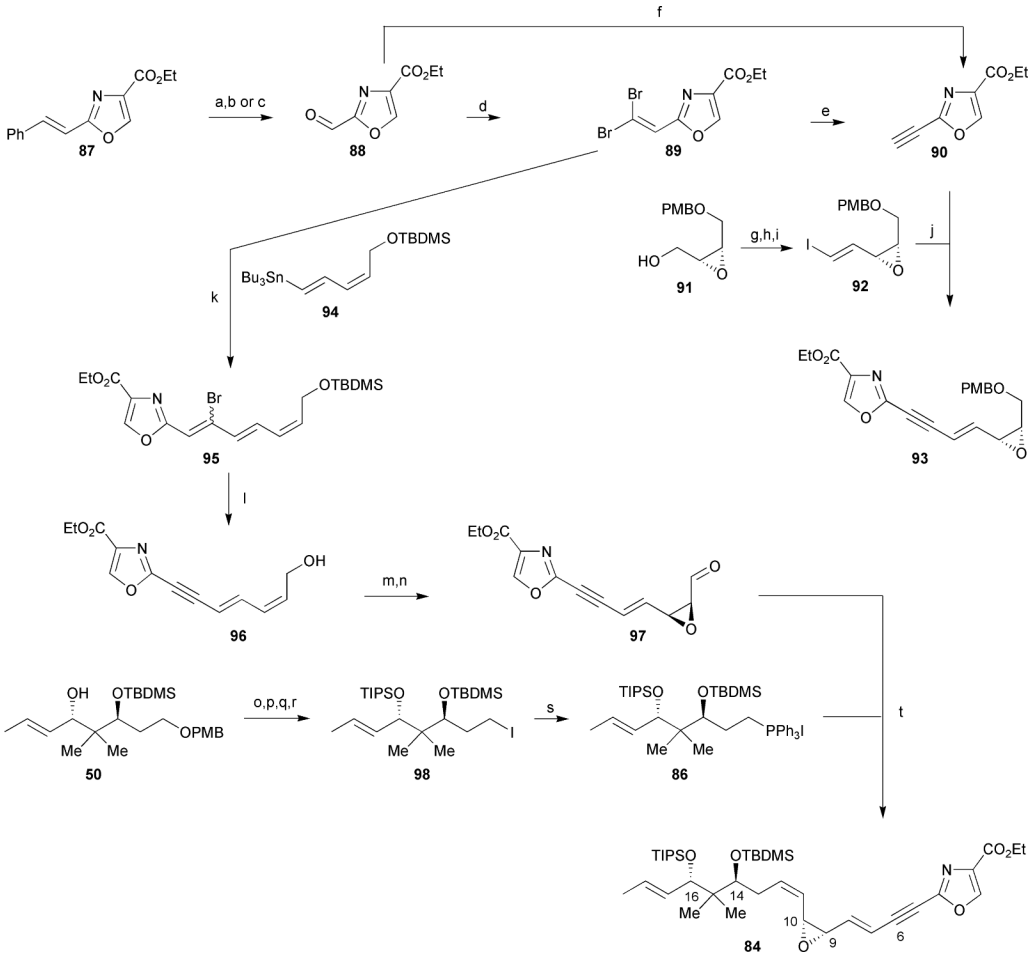

Scheme 13.

Hoffmann's synthesis of a masked northern half of disorazole A_1. *Reagents and conditions*: (a) $K_3[Fe(CN)_6]$, K_2CO_3, OsO_4, $(DHQD)_2PHAL$, *t*-BuOH/H_2O, 96%; (b) $Pb(OAc)_4$, K_2CO_3, benzene, 0 °C, 80%; (c) $NaIO_4$, silica gel, $RuCl_3$·xH2O, CH_2Cl_2, 68%; (d) CBr_4, PPh_3, CH_2Cl_2, 70%; (e) *n*-BuLi, THF, −78 °C, 30%; (f) Ohira–Bestmann reagent **61** (Scheme 7, *vide supra*), K_2CO_3, EtOH, 0 °C to rt, 50%; (g) SO_3·Pyr, Et_3N, CH_2Cl_2/DMSO, 0 °C to rt, 95%; (h) PPh_3, CHI_3, *t*-BuOK, THF, 75%; (i) MeLi, THF, −100 °C, 75%; (j) $PdCl_2(PPh_3)$, CuI, Et_3N, DMF, 15%; (k) **94**, tris(2-furyl)phosphine, Pd_2dba_3, toluene, 100 °C, 86%; (l) TBAF, THF, 0 °C, 87%; (m) D-(−)-diethyl tartrate, $Ti(Oi\text{-}Pr)_4$, *t*-BuOOH, 4Å MS, CH_2Cl_2, −18 °C, 84%; (n) $PhI(OAc)_2$, TEMPO, CH_2Cl_2, 81%; (o) TIPSOTf, 2,6-lutidine, CH_2Cl_2, 99%; (p) DDQ, CH_2Cl_2/H_2O, 0 °C, 99%; (q) MsCl, Et_3N, DMAP, THF, 0 °C, 99%; (r) NaI, $NaHCO_3$, acetone, Δ, 91%; (s) PPh_3, Hünig's base, sealed flask, 85 °C; (t) **86**, LiHMDS, THF, −78 °C to rt, then **97**, HMPA, −78 °C to rt, 43% (from **98**).

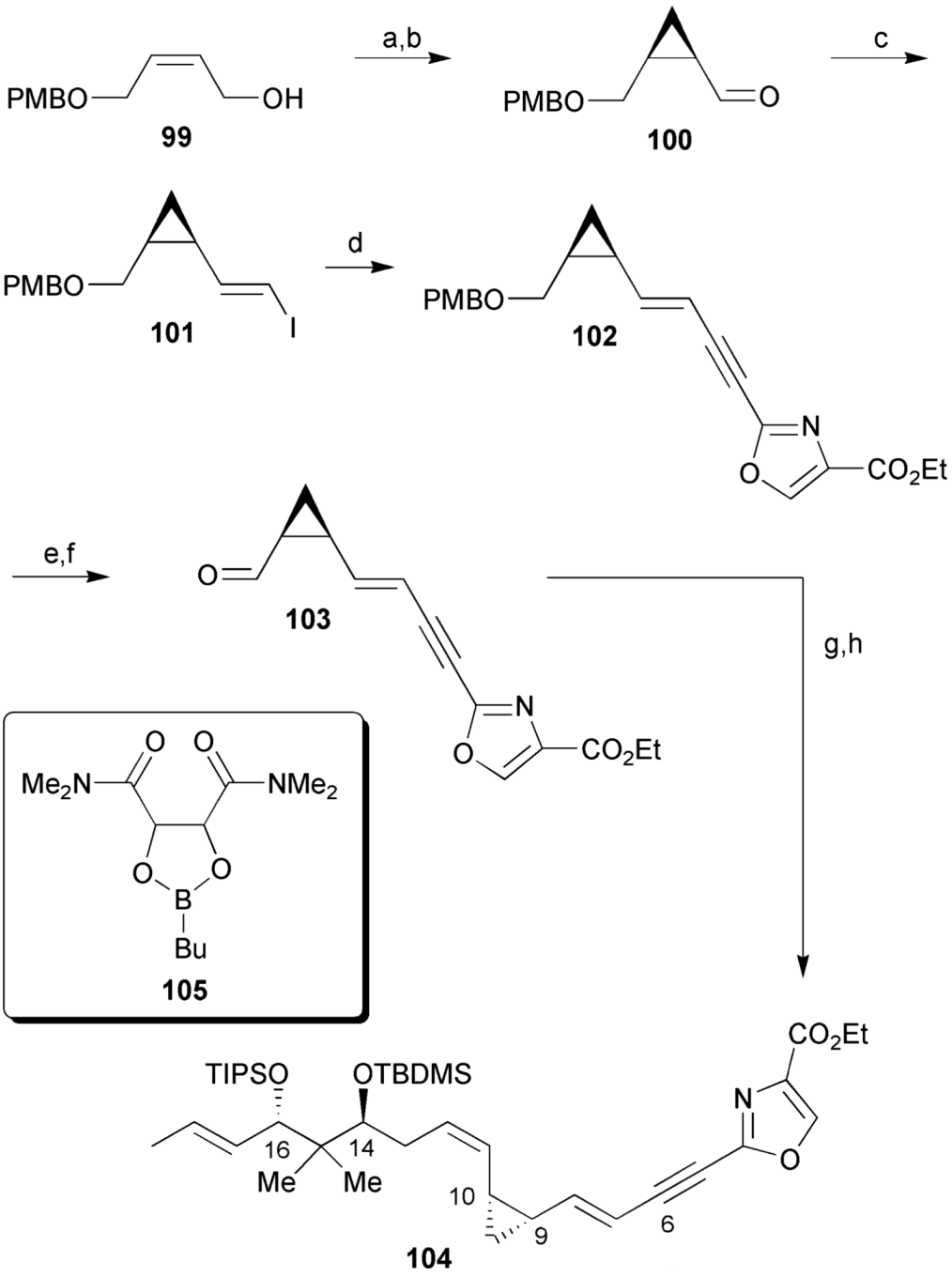

Scheme 14.

Hoffmann's synthesis of a masked cyclopropane analog of the northern hemisphere of disorazole A_1. *Reagents and conditions*: (a) Et_2Zn, CH_2I_2, dioxaborolane **105**, CH_2Cl_2, 0 °C, 81%; (b) Dess–Martin periodinane, $NaHCO_3$, CH_2Cl_2, 88%; (c) $CrCl_2$, CHI_3, THF, 0 °C, 49%; (d) **90**, $PdCl_2(PPh_3)_2$, CuI, Et_3N, DMF, 49%; (e) DDQ, CH_2Cl_2/H_2O; (f) Dess–Martin periodinane, $NaHCO_3$, 72% (over 2 steps); (g) **98**, PPh_3, Hünig's base, 90 °C, then **103**, LiHMDS, HMPA, THF, −78 °C to rt, 40%.

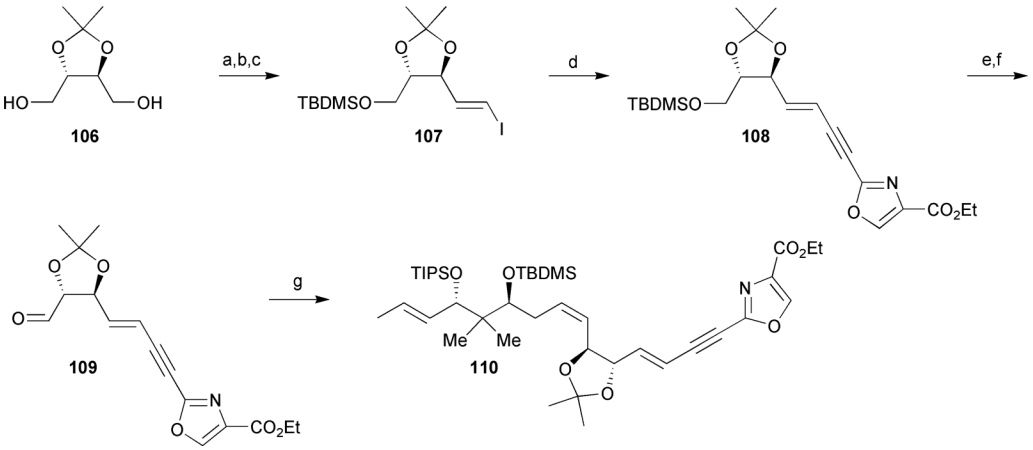

Scheme 15.

Hoffmann's synthesis of a masked northern half of disorazole D_1. *Reagents and conditions*: (a) NaH, TBDMSCl, THF, 85%; (b) SO_3·Pyr, Et_3N, DMSO/CH_2Cl_2, 0 °C, 96%; (c) $CrCl_2$, CHI_3, THF, 72%; (d) **90**, $PdCl_2(PPh_3)_2$, CuI, Et_3N, DMF, 86%; (e) TBAF, THF, 0 °C, 99%; (f) Dess–Martin periodinane, pyridine, CH_2Cl_2, 0 °C, 75%; (g) **86**, LiHMDS, HMPA, THF, −78 °C to rt, 32%.

Table 1

Activity comparison of disorazole A_1, epothilone B, and vinblastine against established animal and human cancer cell lines (data taken from refs [12] and [14]). IC_{50} values refer to antiproliferative activities

		IC_{50} (nM)		
Cell Line	**Origin**	**Disorazole A_1 (1)**	**Epothilone B**	**Vinblastine**
A549	*Human lung carcinoma*	0.0023 ± 0.0005	0.26 ± 0.14	5.9 ± 0.5
PC-3	*Human prostate adenocarcinoma*	0.0071 ± 0.0012	2.0 ± 0.3	0.82 ± 0.06
SK-OV-3	*Human ovary adenocarcinoma*	0.0049 ± 0.0001	0.64 ± 0.07	1.4 ± 0.1
A-498	*Human kidney carcinoma*	0.016 ± 0.004	4.3 ± 3.6	46 ± 12
U-937	*Human histiocytic lymphoma*	0.002 ± 0.001	0.09 ± 0.01	0.43 ± 0.13
K-562	*Human myelogenous leukemia*	0.006 ± 0.001	0.69 ± 0.03	8.7 ± 1.8
KB-3.1	*Human cervix carcinoma*	0.0025 ± 0.0003	1.6 ± 0.6	8.6 ± 0.3
KB-V1	*Human cervix carcinoma (multi-drug resistant)*	0.042 ± 0.008	0.57 ± 0.03	114 ± 31
L929	*Mouse fibroblasts*	0.0038 ± 0.0002	1.3 ± 0.6	28 ± 7

Table 2

Activity comparison of disorazole C_1, vincristine, and vinblastine against established animal and human cancer cell lines (data taken from ref. [26]). IC_{50} values refer to antiproliferative activities

		IC_{50} (nM)		
Cell Line	**Origin**	**Disorazole C_1 (10)**	**Vincristine**	**Vinblastine**
A549	*Human lung carcinoma*	2.21 ± 0.23	21.62 ± 2.68	1.52 ± 0.09
PC-3	*Human prostate adenocarcinoma*	1.57 ± 0.10	4.68 ± 0.29	0.86 ± 0.08
MDA-MB-231	*Human breast epithelial adenocarcinoma*	3.53 ± 0.19	7.16 ± 0.37	1.34 ± 0.21
2008	*Human ovarian carcinoma*	1.91 ± 0.23	21.81 ± 2.92	2.24 ± 0.16
Quiescent WI-38	*Normal lung fibroblast*	>100	N/D	>100
HCT-116 WT	*Human colorectal carcinoma*	1.09 ± 0.41	5.62 ± 0.33	1.40 ± 0.07
HCT-116 p53 −/−	*Human colorectal carcinoma*	2.25 ± 0.71	5.42 ± 0.47	2.17 ± 0.35
DC3F WT	*Chinese hamster lung cancer fibroblasts*	5.55	17.53	
VCRD-5L	*Chinese hamster lung cancer fibroblasts (multi-drug resistant)*	6.77	N/A	